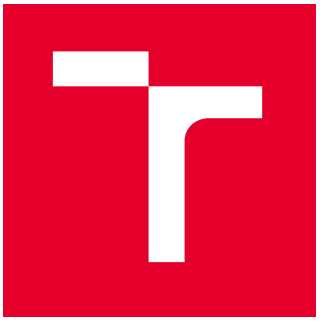

BRNO UNIVERSITY OF TECHNOLOGY

VYSOKÉ UČENÍ TECHNICKÉ V BRNĚ

FACULTY OF CHEMISTRY

FAKULTA CHEMICKÁ

INSTITUTE OF PHYSICAL AND APPLIED CHEMISTRY

ÚSTAV FYZIKÁLNÍ A SPOTŘEBNÍ CHEMIE

MICRO/MACRO-SCALE INVESTIGATION OF THE VISCOELASTIC PROPERTIES OF HYDROGEL MATERIALS

VISKOELASTICKÉ VLASTNOSTI HYDROGELOVÝCH MATERIÁLŮ STUDOVANÉ NA MIKRO/MAKRO ÚROVNI

MASTER'S THESIS

DIPLOMOVÁ PRÁCE

AUTHOR — **Bc. Klára Obrusníková**

AUTOR PRÁCE

SUPERVISOR — **Ing. Jiří Smilek, Ph.D.**

VEDOUCÍ PRÁCE

BRNO 2024

BRNO UNIVERSITY OF TECHNOLOGY
FACULTY OF CHEMISTRY

Assignment Master's Thesis

Project no.:	FCH-DIP1962/2023	Academic year: 2023/24
Department:	Institute of Physical and Applied Chemistry	
Student:	**Bc. Klára Obrusníková**	
Study programme:	Chemistry for Medical Application	
Field of study:	Processes and Materials of Medical Applications	
Head of thesis:	**Ing. Jiří Smilek, Ph.D.**	

Title of Master's Thesis:

Micro/macro–scale investigation of the viscoelastic properties of hydrogel materials

Master's Thesis:

1. A review on the possibility of studying the rheological properties of hydrogel matrices and the correlation of macro and micro approaches.
2. According to the state–of–the–art select suitable instrumental techniques applicable for the study of viscoelastic properties of hydrogel systems.
3. Optimize selected techniques (especially micro) on a model hydrogel matrix.
4. Correlate the results obtained from macro– and micro–rheological techniques.
5. Critically evaluate the work (applicability of selected techniques to the study of hydrogel systems) and draw logical conclusions.

Deadline for Master's Thesis delivery: 29.4.2024:

Master's Thesis should be submitted to the institute's secretariat in a number of copies as set by the dean This specification is part of Master's Thesis

Bc. Klára Obrusníková student	Ing. Jiří Smilek, Ph.D. Head of thesis	prof. Ing. Miloslav Pekař, CSc. Head of department

In Brno dated 1.2.2024

prof. Ing. Michal Veselý, CSc.
Dean

ABSTRACT

This diploma thesis was focused on the comparison of various microrheological methods with macrorheological approach, especially on the characterisation of hydrogels. Dynamic light scattering, fluorescence correlation spectroscopy and optical tweezers were chosen as the microrheological techniques, while oscillatory rheometry was the macrorheological tool. Results from dynamic light scattering and fluorescence correlation spectroscopy for agarose and gellan hydrogels were compared to rheometry and to each other. The values of viscoelastic moduli obtained by microrheology were significantly lower than those obtained by macrorheology. Both dynamic light scattering and fluorescence correlation spectroscopy offer a wider range of frequencies than rheometry, but both have limitations in hydrogel characterisation. In dynamic light scattering measurements, light scattered from hydrogel networks causes noise and lowers the quality of the results. Fluorescence correlation spectroscopy, while being more specific, shows very little difference between samples of different concentrations. Optical tweezers are a new method at the Faculty of chemistry, and only the calibration measurements were performed. Optical trap stiffness, an important value in the calibration process of optical tweezers, was determined for solutions of glycerol.

ABSTRAKT

Tato diplomová práce byla zaměřená na srovnání mezi mikroreologickými metodami a makroreologickým přístupem, zejména při charakterizaci hydrogelů. Dynamický rozptyl světla, fluorescenční korelační spektroskopie a optická pinzeta byly vybrány jako mikroreologické techniky, zatímco oscilační reometrie sloužila jako makroreologický nástroj. Výsledky z dynamického rozptylu světla a fluorescenční korelační spektroskopie pro hydrogely agarózy a gellanu byly porovnány s reometrií a mezi sebou. Hodnoty viskoelastických modulů získané z mikroreologických měření byly výrazně nižší než ty získané pomocí makroreologie. Jak dynamický rozptyl světla, tak fluorescenční korelační spektroskopie nabízejí širší škálu měřitelných frekvencí než reometrie, ale obě metody mají své limitace při charakterizaci hydrogelů. U dynamického rozptylu světla dochází k odrazu světla od gelové sítě, což způsobuje šum a zhoršuje kvalitu získaných výsledků. Fluorescenční korelační spektroskopie, přes svou vyšší specifitu, vykazuje jen velmi malé rozdíly mezi vzorky různých koncentrací. Optická pinzeta je na Fakultě chemické novou metodou, a byla provedena pouze kalibrační měření. Tuhost optické pasti, důležitá hodnota pro kalibraci optické pinzety, byla stanovena pro roztoky glycerolu.

KEYWORDS

Rheology, microrheology, fluorescence correlation spectroscopy, dynamic light scattering, optical tweezers, hydrogels

KLÍČOVÁ SLOVA

Reologie, mikroreologie, fluorescenční korelační spektroskopie, dynamický rozptyl světla, optická pinzeta, hydrogely

OBRUSNÍKOVÁ, Klára. *Viskoelastické vlastnosti hydrogelových materiálů studované na mikro/makro úrovni.* Brno, 2024. Dostupné také z: https://www.vut.cz/studenti/zav-prace/detail/156928. Diplomová práce. Vysoké učení technické v Brně, Fakulta chemická, Ústav fyzikální a spotřební chemie. Vedoucí práce Jiří Smilek.

PROHLÁŠENÍ

I declare that the diploma's thesis has been worked out by myself and that all the quotations from the used literary sources are accurate and complete. The content of the diploma thesis is the property of the Faculty of Chemistry of Brno University of Technology, and all commercial uses are allowed only if approved by both the supervisor and the dean of the Faculty of Chemistry, BUT.

.....

Klára Obrusníková

Acknowledgments:

First of all, I would like to thank my supervisor, Ing. Jiří Smilek, Ph.D., and Ing. Martin Kadlec, for all their time, insightful feedback, advice and support. Further, I would like to acknowledge Ing. Michal Kalina, Ph.D., Ing. Kateřina Marková, Ing. Mojmír Šerý, Ph.D. and Ing. Petr Jákl, Ph.D., for all their assistance and advice with the measurements.

Finally, I am grateful to my family and friends for all their support throughout my university studies. It would not have been possible without you.

TABLE OF CONTENTS

1 INTRODUCTION

Hydrogels are an emerging class of materials with diverse applications in various fields like biotechnology, food industry or medicine. They offer some unique and convenient properties, like their capability of holding large amounts of water, their biocompatibility or versatility.

Hydrogels are viscoelastic solids with a complex rheological behaviour. Their specific applications could require a thorough understanding of their rheological properties in different conditions. In tissue engineering, for example, matching the properties of living tissues, including their rheological behaviour, is critical.

This thesis focuses on the comparison of two rheological principles. Macrorheology, a common method used to determine rheological properties on the macroscopic scale. And microrheology, which explores the local rheological properties on a microscopic scale, potential inhomogenities, and their influence on macroscopic behaviour.

Three different microrheological techniques were chosen for the comparison, namely dynamic light scattering, fluorescence correlation spectroscopy and optical tweezers. Each technique provides a different approach, different advantages and limitations, and each can provide a different insight into the complex rheological behaviour of hydrogels. The comparison, not only between the macro and micro approaches, but also between the microrheological methods, could deepen the understanding of rheological properties and how to tailor them best to a specific application.

2 THEORETICAL PART

2.1 Macrorheology

In elementary physics, a material is either solid or liquid. Reality is, however, much more complex and few things fit the definitions of "ideal" states of matter. Between an ideal solid and an ideal liquid, there is a variety of materials from different fields, that cannot be easily classified as one of those. That is the reason why rheology was established as a separate field of science in 1929, when the American Society of Rheology was founded. Definition of rheology is "*the study of the deformation and the flow of matter*". That is reflected in the term itself, which comes from the Greek words "*rhei"*, meaning to flow, and "*logos"*, meaning science [1].

Rheology primarily deals with viscoelastic materials, which exhibit a mixture of viscous and elastic behaviour. Ideally viscous liquids and ideally elastic solids are described by Newton's and Hooke's laws. Viscoelastic liquids and solids can be found in different areas, for instance the food industry (ketchup, dough), construction (paints, asphalt), biology and medicine (blood, tissues, hydrogels) [2].

Ideally viscous liquids are described by Newton's law of viscosity, and therefore called Newtonian fluids. For the definition of viscosity, simple two-plate model in shear can be used. The lower plate is stationary, while the upper plate moves parallel to the lower plate. A sample is applied between those two plates and the upper plate is set in motion by force *F* [N].

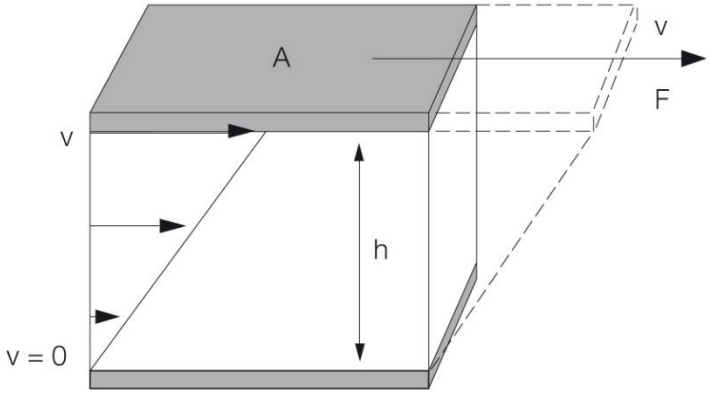

Figure 1 Two-plate model used for the definition of viscosity [3]

Shear stress τ [Pa] is defined as force *F* applied to the area of the plate *A* [m^2].

$$\tau = \frac{F}{A} \tag{1}$$

As the result of the upper plate moving with the velocity *v* [m/s], while the lower plate is stationary (its velocity is zero), the sample moves in individual layers. Close to the upper plate, the sample velocity equals *v*, close to the lower plate, the sample velocity equals zero. The velocity gradient, or shear rate $\dot{\gamma}$ [s^{-1}], is defined as

$$\dot{\gamma} = \frac{v}{h} \tag{2}$$

where h [m] is the gap between the two plates [2].

Having defined shear stress and shear rate, Newton's law can be formulated. Newton's law establishes a relation between shear stress and shear rate through viscosity η [Pa·s].

$$\tau = \dot{\gamma} \cdot \eta \tag{3}$$

For Newtonian fluids, viscosity is a material constant, not dependant of shear stress, only temperature and pressure. It is a unique material characteristic, expressing the inner friction of a fluid and its resistance against flow. Viscosity is defined on the premise of laminar flow when layers move parallel to each other without the occurrence of vortices. Apart from dynamic viscosity η, kinematic viscosity ν [m^2/s] also exists, defined as dynamic viscosity divided by density ρ [kg/m^3]. In contrast to experiments where shear is the driving force and dynamic viscosity is obtained, kinematic viscosity is determined in experiments in which gravity (or the weight of the sample) is the driving force [4].

$$\nu = \frac{\eta}{\rho} \tag{4}$$

Newtonian fluids are generally dilute solutions and solutions of low molecular weight substances, like water or milk. Other fluids can undergo changes in viscosity either according to applied shear rate or in time. These are called non-Newtonian fluids and can be further distinguished by their flow and viscosity curves. A flow curve expresses the relation between shear stress and shear rate, a viscosity curve expresses how viscosity changes with applied shear rate.

Shear-thinning fluids, also called pseudoplastic, are those whose viscosity decreases with increasing shear rate. Shear-thinning behaviour is typical for polymer solutions. Viscosity decreases due to changes in fluid's internal structure that lead to decreased resistance against flow, therefore decreased viscosity. Those changes include untangling of molecules that are entangled at rest, orientation of molecules in the direction of shear, while their arrangement is random at rest, or breakage of loose bonds between particles forming agglomerates. Shear-thinning is a favourable property because it lowers the energy needed for mixing or transporting fluids [4].

The opposite behaviour, increase in viscosity with increasing shear rate, is called shear-thickening or dilatant. Shear-thickening materials include highly concentrated dispersions or ceramic suspensions. It is, however, a rarer and less favourable property, as it can complicate technical processes and cause problems with stirring or spraying [4].

A Bingham fluid is a fluid that flows independently of shear rate (viscosity is constant), but only after a certain shear rate value is exceeded. The limit value of shear rate is called yield stress. Bingham fluids can be found in various fields and in everyday life, for example toothpaste, mayonnaise, ketchup, some paints or cosmetics [5].

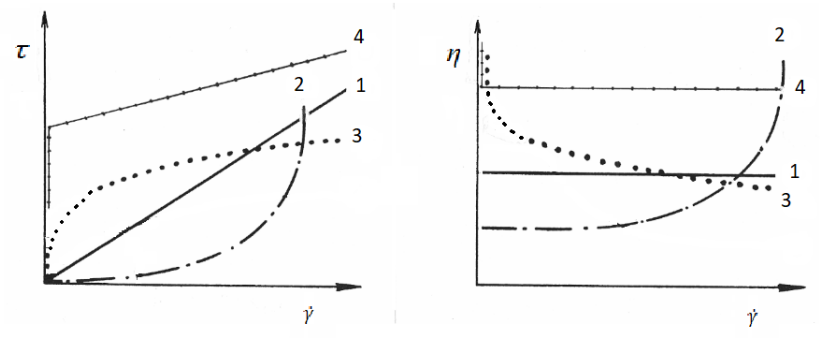

Figure 2 Flow and viscosity curves of a Newtonian (1)*, shear-thinning* (2)*, shear-thickening* (3) *and Bingham* (4) *fluid [4]*

Other than shear deformation, viscosity of some non-Newtonian fluids can also be dependent on time of applied shear. This property is called thixotropy or rheopexy, depending on the specific effect. Thixotropy is a continuous decrease in viscosity induced by a force, that is applied to a sample and causes it to flow. When the force is discontinued and the sample rests, viscosity returns to its previous value – the effect is reversible. The decrease in viscosity is caused by changes in microstructure. The forces within the sample, holding its structure together, are weak enough to be broken by mechanical stress, but will rebuild when the stress is removed. Many shear-thinning materials are also thixotropic, for example paints, inks, gels or bone cements [6]. The opposite effect is called rheopexy, which means an increase in viscosity when shear is applied. Rheopexy is a rarer property than thixotropy. Synovial fluid or albumin solutions are rheopectic, due to protein aggregation caused by shear [7].

Similarly to the law of viscosity, law of elasticity, or Hooke's law, defines ideally elastic behaviour for solids. Hooke's law states that for relatively small deformations, the size of the deformation is proportional to the deforming force. Upon removal of this force, the object returns to its original size and shape. Briefly, stress is proportional to strain. The ratio between applied stress and produced strain is called Young modulus [8].

2.1.1 Viscoelasticity

Many materials do not exhibit fully viscous or fully elastic behaviour, but a combination of both, defined as viscoelastic behaviour. Viscoelasticity is an important concept in rheology, as was said previously. Whether a substance behaves more like an elastic solid or like a viscous liquid can be dependent on the timescale of the observed process, which is expressed by Deborah number. Deborah number is defined as

$$D_e = \frac{\tau}{T} \tag{5}$$

where τ [s] is a characteristic time of a material (time it takes the material to adjust to applied deformation) and T [s] is the time of the deformation process that is being observed. For ideal solids, τ is infinite, and for ideal liquids, τ is zero [1]. Demonstration of this concept, that even a material that appears as a solid can flow if given enough time, is the famous pitch drop experiment. It has been running since 1927, and a drop takes around a decade to fall [9].

To define necessary terms and grasp the concept of viscoelasticity, the two-plate model can be used again. When force is applied, the upper plate moves. If the movement is stopped and

the deflection path s [m] is defined, then the shear strain γ [-] is the ratio between s and the gap between the two plates h:

$$\gamma = \frac{s}{h} \tag{6}$$

Shear strain is a dimensionless number expressing the deformation, usually stated as a percentage. Previously defined shear stress τ is related to shear strain through shear modulus G [Pa].

$$\tau = G \cdot \gamma \tag{7}$$

When measuring viscoelastic behaviour, this principle of having a stationary lower plate while the upper plate moves in a defined path is used in oscillatory tests. The upper plate moves back and forth, oscillating around the equilibrium position with oscillatory frequency f [Hz] and strain γ. Strain plotted against time results in a sine curve. Same applies for shear stress that is evaluated as the counterforce used to keep the lower plate stationary. These two sine curves oscillate with the same frequency f, and for an ideal solid, there is no phase shift between them. For viscoelastic materials, however, shear stress and strain oscillate with a phase shift δ [°] which is illustrated in Figure 3. The phase shift is between 0° and 90°, while 0° is the value for an ideal solid and 90° for an ideal liquid [2].

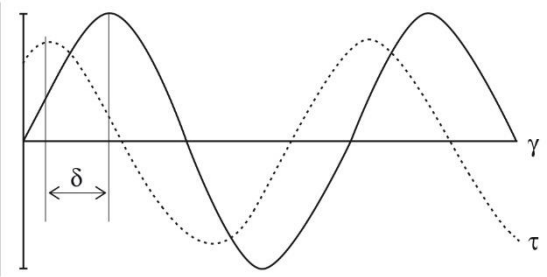

Figure 3 Shear stress and strain plotted against time [3]

The shear stress amplitude τ_A and strain amplitude γ_A are related through the complex shear modulus G^* [Pa], which describes viscoelastic behaviour, as in equation 7.

The complex shear modulus consists of two parts, real and imaginary. The real part is the storage (or elastic) modulus G', and the imaginary part is the loss (or viscous) modulus G''. The elastic portion, storage modulus, represents the part of the deformation energy that is stored, while the viscous portion, loss modulus, represents the part of the energy that is dissipated through internal friction.

$$G^* = G' + \mathrm{i}G'' \tag{8}$$

The values of the moduli can be determined using the following equation, based on the Pythagoras theorem and the relationship between the moduli represented in Figure 4.

$$G^* = \sqrt{G'^2 + G''^2} \tag{9}$$

Storage and loss moduli are determined by the phase shift angle δ. The relationship between the moduli and the angle can be described by following equation or graphically, as in Figure 4. The ratio between storage and loss modulus, $\tan\delta$, is called the loss factor. For ideally elastic behaviour, the loss factor equals zero ($\delta = 0°$), while for ideally viscous behaviour, the loss factor approaches infinity ($\delta = 90°$) [2].

$$\tan\delta = \frac{G''}{G'} \tag{10}$$

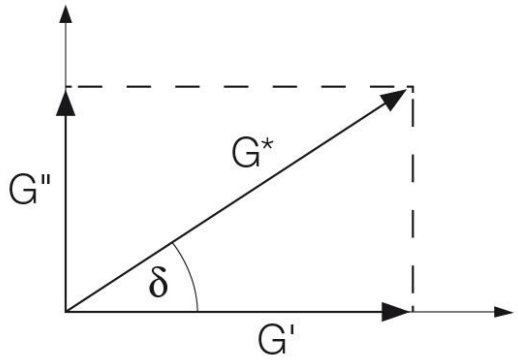

Figure 4 Relationship between complex, storage, and loss modulus [3]

Another viscoelastic characteristic is the creep compliance J [Pa^{-1}]. It can be determined by measuring strain response under constant stress. The ratio of the measured strain and the applied stress gives J, which can also be written as inverted complex modulus [10].

$$J = \frac{\gamma}{\tau} = \frac{1}{G^*} \tag{11}$$

2.1.2 Rheometry

The experimental part of rheology is called rheometry. It is used to measure rheological behaviour (flow, deformation) of materials under the influence of applied force. For measuring viscosity, viscosimeters can be used. To determine more complex properties or flow curves, rheometers are needed.

On a rheometer, based on the character of the sample, different measuring geometries can be used. Either concentric cylinders, which are more suitable for fluid materials with lower viscosity, or cone/plate and plate/plate geometries, more suitable for viscoelastic solids. Cone/plate geometry provides a slightly more precise measurement since the shear conditions are uniform in the entire gap – in the plate/plate geometry, shear rate at the edge of the plate is higher than at the centre. However, plate/plate geometry offers the possibility of profiled surfaces that prevent sample migration, which is useful for materials like hydrogels [2].

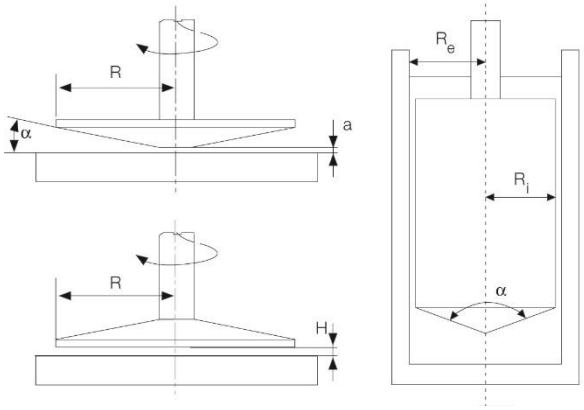

Figure 5 Types of measuring geometries [3]

According to the type of movement the sensor does, rotational and oscillatory tests can be distinguished. In rotational tests, the upper geometry rotates with a certain shear rate and the dependence of viscosity on shear rate (flow curve) is measured. Oscillatory tests are more appropriate for measuring viscoelastic behaviour. The upper geometry oscillates around an equilibrium position with a certain frequency and strain. Either amplitude sweeps (strain or stress sweeps) or frequency sweeps can be performed. In an amplitude sweep, frequency is a constant while the deflection of the geometry (strain) changes. The linear viscoelastic (LVE) region is determined by this type of tests. Frequency sweeps provide information about time-dependent behaviour of materials. The frequency is changing, and strain is held constant, in the range of the LVE region, which means the deformation is non-destructive [2].

Time-temperature superposition

Time-temperature superposition (TTS) is a principle that can be used in rheometry to extend the oscillation frequency range. Normally, only a frequency of 100 Hz can be reached by rheometry, but it could be less based on the raw phase angle (phase shift between displacement and torque signal), which indicates the limits of a rheometer. The broader frequency range is reached by shifting frequency-dependant data obtained at several different temperatures to a reference temperature. TTS is valid for so-called termorheologically simple materials. By shifting the obtained viscoelastic functions (such as complex viscoelastic modulus) vertically and horizontally, a master curve is generated [11].

2.2 Microrheology

Microrheology is a technique used for studying the viscoelastic properties of materials on a micro-scale. The basic principle of microrheology is using a tracer inserted in the sample and a tool to detect its motion [12].

Two main classes of techniques can be distinguished when talking about microrheology. In case that the motion of the particle is driven solely by thermal fluctuation, then we talk about passive microrheology. In passive microrheological techniques, the *mean-square displacement* (MSD) of particles is measured as a function of lag time. If the motion is induced by an external force, then it is called active microrheology. In this case, the response of the particle to the applied force is measured [12].

MSD is the key outcome of microrheological measurements. It is defined in three dimensions as

$$\langle \Delta r^2(\tau) \rangle = \langle [x(t+\tau) - x(t)]^2 + [y(t+\tau) - y(t)]^2 + [z(t+\tau) - z(t)]^2 \rangle \quad (12)$$

where t is time, τ is the lag time and x, y and z [m] represent position data. In a purely viscous medium, MSD of a particle will increase linearly with time. In a purely elastic material, on the other hand, MSD will not increase at all, as the particle would only oscillate around an equilibrium position. For viscoelastic materials, MSD can be measured over time and the result would be equivalent to viscoelastic properties as a function of frequency [13].

MSD is derived to complex modulus through generalized Stokes-Einstein relation (GSER).

$$\tilde{G}(s) = \frac{k_B t}{\pi a s \langle \tilde{r}^2(s) \rangle} \quad (13)$$

where s is the Laplace frequency, $\langle \tilde{r}^2(s) \rangle$ is the Laplace transform of MSD, and $\tilde{G}(s)$ is the viscoelastic spectrum as a function of Laplace frequency. Quantifying the viscoelastic moduli is possible through numeric methods [13].

One way to get viscoelastic moduli from MSD is through creep compliance J, which is linearly related to MSD [14]:

$$J = \frac{\pi a}{k_B T} \langle \Delta r^2(t) \rangle \quad (14)$$

Once creep curves are obtained, a retardation spectrum can be calculated by fitting a model, and then calculating G' and G'' [14].

Microrheology offers some essential advantages over “classic” macrorheology. It requires significantly smaller volume of the sample, which can be useful especially with rare or expensive materials, including biological samples like cells, or for studying newly synthetised materials. Microrheology also measures viscoelastic properties locally, which means it can be used to study heterogeneities within the sample. Another advantage is a far greater range of frequencies that can be reached without the use of time-temperature superposition (TTS), described in chapter 2.1.2. There are, however, problems when comparing micro and macrorheological results. One reason for inconsistency between results can be improper choice of probe size. If the results of a microrheological experiment are interpreted using GSER, for them to be valid, the probe that is used should be significantly larger than the relevant microstructure of the studied material (e.g. pore or mesh size, entanglement length). If the probe is too small, it diffuses freely and only the viscous properties of the solvent are probed, not the viscoelasticity of the whole material. Another problem can be an interaction between the material and the probe (electrostatic interaction, chemical binding), which can alter the local environment and therefore the measured mechanical properties [15].

2.2.1 Particle tracking

One of the most fundamental passive microrheological tools is particle tracking microrheology (PTM) or multiple particle tracking microrheology (MPT). This method relies on simply tracking the Brownian movement of a particle by taking a video and analysing its trajectory [16].

Brownian motion is random and driven by thermal energy. MSD of the bead can be related to the diffusion coefficient D [m^2/s]:

$$\langle \Delta r^2 \rangle = 4Dt \tag{15}$$

For spherical particles, diffusion coefficient is related to viscosity by Stokes-Einstein relation, and therefore for viscous liquids, measuring MSD is sufficient to obtain their viscosity η.

$$D = \frac{k_B T}{6\pi\eta r} \tag{16}$$

In case of a viscoelastic material, the viscoelastic modulus can be calculated from MSD by GSER, as mentioned in the previous chapter.

In MPT, a large number of particles is tracked to ensure an adequate statistical averaging of their trajectories. MPT provides simple and rapid measurements of viscoelastic properties without subjecting the measured material to a force, as it relies only on thermal fluctuations. That makes it suitable, for example, for measurements inside living cells [16].

2.2.2 Dynamic light scattering

Dynamic light scattering (DLS) is a technique used to determine the size of particles by measuring their Brownian motion. Particles in a solvent move randomly due to collisions with the solvent molecules surrounding them. This motion depends on solvent viscosity, temperature (since viscosity is strongly dependant on temperature), and size of the particles. Large particles move slower than smaller particles, therefore it is possible to determine their size by measuring their movement [17].

In DLS, a monochromatic beam of light shines on the sample contained in a cuvette and gets scattered. The scattered light is detected at a certain angle over time. Intensity fluctuations of the scattered light are analysed, and the diffusion coefficient and particle size are obtained. The difference from static light scattering (SLS), a similar technique, is that in SLS, the time-average intensity of scattered light is analysed, and molecular weight and radius of gyration are obtained [17].

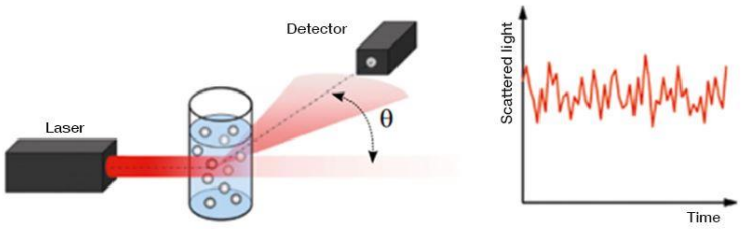

Figure 6 Schematic experimental setup of DLS [18]

DLS microrheology

The principle of microrheology is detecting the motion of a tracer within the sample. That makes DLS, a method based on detecting motion of particles, a useful microrheological tool. Fluctuations in probe scattering intensity are measured, and the autocorrelation function is formed. From the autocorrelation function, MSD of the probe is derived, and viscoelastic moduli are determined using GSER [17].

DLS is a common and simple method offering measurements in a broad range of frequencies. It is nondestructive, which allows for rheological measurements of time-dependant systems, such as sol-gel transitions or remodelling of extracellular matrix. The nondestructivness also allows for measurements of delicate systems like cells. There are, however, some limitations in microrheological experiment via DLS. Only transparent samples can be measured via DLS. Proper dispersion of probe particles is critical because their radius is used in the analysis, meaning aggregates can disrupt the results. This is important especially in gels, where the particles need to be dispersed before gelation [19, 20].

2.2.3 Fluorescence correlation spectroscopy

Fluorescence correlation spectroscopy (FCS) is a technique used to study kinetic processes through the statistical analysis of intensity fluctuations from equilibrium. It was first developed in the 1970s by Madge, Elson and Webb [21] to study the intercalation of ethidium bromide (EtBr) to double-stranded DNA by measuring the fluorescence fluctuations of EtBr. During the first measurements, the method had poor signal-to-noise ratios, caused by low detection efficiency, large observation volumes and insufficient background suppression. With the combination of highly focused laser and a pinhole, a very small confocal observational volume was created. In addition, ultrasensitive detectors with single-photon sensitivity and efficient fluorescent labelling dyes have helped the breakthrough of this method. Nowadays, FCS is considered a standard laboratory technique and a powerful tool for colloid characterization [23].

The typical setup of FCS resembles a classical confocal microscope, its schematic representation is depicted in Figure 7. A laser beam is focused through a microscope objective, which is typically immerse. The excited fluorescence light is collected and passes through a dichroic mirror and emission filter. The light is imaged onto a confocal pinhole, blocking any light that does not originate from the focal region, which creates a very small observation volume. The light is then focused onto the detector, which can be an avalanche photodiode or a photomultiplier [24].

The fluctuations in detected fluorescence intensity are recorded and analysed by an autocorrelation function. Those fluctuations are caused by fluorescent probes diffusing through the confocal volume. From the autocorrelation function and the size of the observed confocal volume, diffusion coefficients of the fluorescent probes are obtained. The autocorrelation function $G(t)$ gives information about the average number of fluorescent species in the observed volume (N) and the diffusion time τ_D, which is related to the diffusion coefficient D through the following equation, where r_0 is the radius of the confocal volume [24]:

$$\tau_D = \frac{r_0^2}{4D} \tag{17}$$

The autocorrelation function is related to MSD by following equation, where w_{xy} and w_z define the dimensions of the confocal volume [22]:

$$G(t) = \frac{1}{N}\left(1 + \frac{2}{3w_{xy}^2}\langle \Delta r^2(t)\rangle\right)^{-1}\left(1 + \frac{2}{3w_z^2}\langle \Delta r^2(t)\rangle\right)^{-1/2} \quad (18)$$

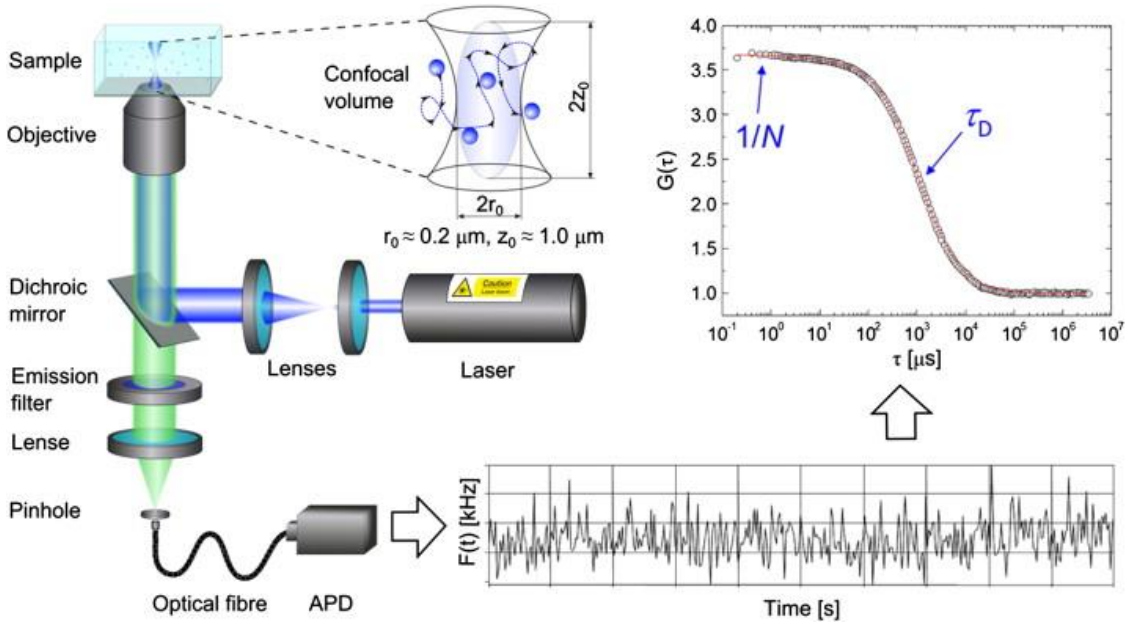

Figure 7 Schematic representation of FCS setup and its principle [24]

FCS provides some unique properties, which make it advantageous over other methods. The concentration of fluorescent probes can be (and should be) very low. The size of the probes can vary from 1 up to 500 nm, and a wide range of diffusion coefficients can be measured. The confocal volume can also be placed in specific places in the measured system, which allows measurements of heterogenous materials. However, FCS also has its limitations. The exact dimensions of the confocal volume are essential for precise measurements; therefore, they have to be determined by calibration measurements of fluorescent dyes with known diffusion coefficients. Autofluorescence of samples can cause interference and poor signal quality, so the probe must be carefully chosen in fluorescent samples [24].

FCS is a powerful tool with many diverse applications. Those include determining diffusion coefficients, measuring the kinetics of chemical reactions, enzyme kinetics, molecular interactions or conformational changes [23]. Apart from those, other uses of FCS may be possible in the future. One could be monitoring nonequilibrium steady states in living cells on molecular level. It is, however, impossible to estimate the advancement of a method that is already so vastly used in biology, chemistry and biotechnology [25].

2.2.4 Optical tweezers

Optical tweezers (OT) are a tool capable of measuring rheological properties which can be used in various experiment designs in many fields. A beam of laser light is focused through a microscope objective lens. This laser beam produces small optical forces, which can be used to weakly trap and manipulate dielectric microscopic objects suspended in a fluid. It is a non-invasive method studying individual molecules [26].

The concept of optical tweezers was first introduced by Arthur Ashkin in the 1970s, when he suggested the possibility of trapping small objects by radiation pressure. The same author then constructed the first optical trap in 1986, that was able to stably hold dielectric particles ranging in size from 10 μm to only 26 nm. Askin suggested future prospects of this method in trapping colloidal particles, macromolecules, polymers and even biological particles. The broad current and potential applications of optical tweezers confirm the relevance of this discovery [27].

The varying research fields and their usage of this method are collected in a thorough review Roadmap for optical tweezers [28]. The broad range of applications of optical tweezers include fields like life sciences, physics, biophysics or engineering, and as a prospect, space exploration. They can be used to measure forces at the femtonewton level, for microrheology of complex fluids or single-cell analysis.

Optical tweezers microrheology

Combining optical tweezers with a probe-position detector (which can be a camera or a quadrant photodiode) gives access to a time-dependant trajectory of a tracer, which is the aim of a microrheological experiment.

An important variable in an experiment with OT is the optical trap stiffness κ [N/m]. It can be determined with the use of equipartition theorem, relating the bead position to thermal energy:

$$\frac{d}{2} k_B T = \frac{1}{2} \kappa \langle r_j^2 \rangle \tag{19}$$

$\langle r_j^2 \rangle$ is the time-independent variance of the Cartesian component (j = x, y, z) of the d-dimensional vector describing the displacement of the trapped particle from the trap centre, k_B is Boltzmann constant, and T is temperature. This method of determining the trap stiffness is independent of the viscoelastic properties of the studied fluid, making it suitable for calibration [29].

After calibrating the optical trap, viscosity of the fluid can be measured by monitoring the displacement of the bead under constant external flow of the surrounding fluid. Balancing the forces between the drag on the bead (based on Stokes relation) and the force of the trap gives following equation:

$$\kappa \cdot \Delta x = 6\pi\eta r v \tag{20}$$

where x is the displacement of the particle from the optical trap centre, r is the radius of the bead, v is the velocity of the fluid (which corresponds to the velocity of the stage) and η is the measured viscosity [30].

For the characterisation of viscoelastic materials, the motion of the particle (MSD) needs to be converted to viscoelastic moduli. When interpreting the elastic modulus, the elastic behaviour of the trap itself must be taken into account. The true storage modulus G' is calculated from the observed storage modulus G'_{obs} by subtracting the elastic contribution of the trap [30]:

$$G' = G'_{obs} - \frac{\kappa}{6\pi r} \tag{21}$$

To obtain results from OT measurements, the position of the probe needs to be acquired from the raw data. If a camera is used as the detector, this means using a tracking algorithm to obtain positions from an image sequence. The displacements of particles occur on a nanometer scale, and typically, pixel sizes range between 30 and 150 nm. That means the tracking algorithm must determine the positions on a sub-pixel level. Different approaches exist, such as centroid or correlation-based methods. Centroid-based methods rely on setting a threshold and then calculating the centre of mass of the tracked object in each image. Correlation-based methods rely on algorithms to locate the particle of interest by comparing each image to a template [31].

2.3 Hydrogels

Hydrogels are a class of materials with unique properties, which make them useful in a wide range of applications. Hydrogels can be made from polymers or colloidal clusters by crosslinking and forming a three-dimensional structure. Due to the presence of hydrophilic groups, these networks can absorb large amounts of water and swell. The high water content makes hydrogels soft and flexible and gives them resemblance to living tissue [32].

Both naturally occurring and synthetic polymers can be used to make hydrogels. Natural hydrogels are usually biocompatible, bioactive, and biodegradable, but lack stability and mechanical strength. Some polymers that form hydrogels are collagen, chitosan, agarose, alginate, and many more. Synthetic hydrogels, on the other hand, are made from polymers prepared by polymerising a monomer, such as polyvinyl alcohol (PVA), polyethylene glycol (PEG) or polyacrylic acid (PAA). They are stable and have mechanical strength, but only a few are biocompatible. To combine the advantages of both, semi-synthetic hydrogels are being developed from either a combination of a natural and a synthetic polymer or from chemically modified natural polymers [32].

The polymer network can be held together either by physical entanglements and weak interactions (hydrogen bonds, electrostatic interactions, hydrophobic forces), or by chemical bonds. Based on this, physical or chemical gels are distinguished. Physical interactions are reversible and can be disrupted by changing the physical conditions (pH, ionic strength, temperature, addition of solutes competing for affinity). Chemical hydrogels are generally more stable and stiffer [33].

2.3.1 Medical applications

Hydrogels have been used in medical applications since the 1960s, when contact lenses were first developed by Otto Wichterle from poly-2-hydroxyethyl methacrylate (pHEMA) [34]. Since that, other hydrogels have been synthetized and specifically tailored to match the desired application. Those include drug delivery systems, wound dressing, or tissue engineering.

Hydrogel delivery systems have found their place in controlled drug administration, thanks to their tunable properties, degradability, and ability to protect drugs from degradation. Controlled drug delivery improves drug efficacy, lower dosage is needed to reach the same outcome and the side effects are less severe. Hydrogels can serve as a platform in which drugs

are encapsulated and later released. Their stiffness can vary to match different tissues in the human body, and their high water content makes them suitable for binding of hydrophilic drugs. The release of the drug can be done by degradation of hydrogel network or by swelling, both increasing the mesh size and allowing the drug to diffuse out of the hydrogel. Another approach is mechanical deformation, which can generate pulsatile release [35].

Another field in which hydrogels are widely used is wound healing. A wound dressing covers the wound and provides a temporary barrier against infections, and also enhances the process of healing. A suitable wound dressing needs to be nontoxic and anti-inflammatory, retain moisture to help maintain the moist environment of the wound, have sufficient mechanical strength to avoid the intrusion of bacteria, and promote cell adhesion, proliferation, and differentiation. That is why hydrogels are excellent candidates. Many polymers, such as gelatin, chitosan or hyaluronic acid and many more, are being studied to construct functional hydrogels. These could combine various functions by being antibacterial, hemostatic, anti-oxidant, anti-inflammatory, self-healing, stimulus responsive or conductive [36].

In tissue engineering, hydrogels are used as scaffolds accommodating living cells. Advantages of hydrogels include their water content, making them a suitable environment for cells and enabling transport into and from cells. They are usually biocompatible and can be easily modified for cell adhesion. However, there are also some limitations, including mechanical weakness or difficulty with handling and sterilising [33].

2.3.2 Agarose

Agarose is fraction of a polysaccharide called agar, which is found in red seaweeds. The other fraction, agaropectin, has charged substituents (sulphate, pyruvate), while agarose is mainly uncharged, although some sugar units could be substituted with charged groups. Agarose forms thermoreversible gels which melt at 80 to 90 °C and solidify at 30 to 40 °C, depending on the exact type [37, 40]. Agarose has wide applications in biochemistry and medicine. It serves as the gel matrix in electrophoresis, an effective method used for separating nucleic acid fragments according to their size. Nucleic acids are negatively charged and migrate to the positively charged anode through the gel matrix when placed in an electric field. The molecular sieving capacity and effectiveness of separation can be modified by changing the concentration, and therefore the pore size, of the agarose gel [38]. Due to its biocompatibility, agarose is also a suitable polymer for drug delivery systems. The porous structure of agarose makes it possible for the embedded drug transport, and the uniform structure allows controlled release [39]. The resemblance of the structure of agarose to the extracellular matrix makes it a good candidate for applications in tissue engineering. It can be used, in combination with other biopolymers, as a scaffold for cartilage regeneration, bone regeneration or as a wound dressing [40].

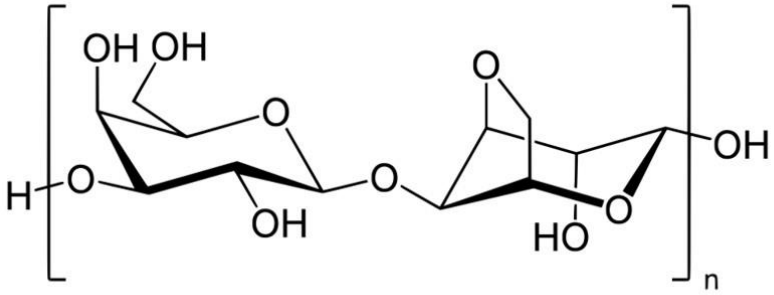

Figure 8 Chemical structure of agarose [41]

2.3.3 Gellan

Gellan is also a natural polysaccharide, produced by the bacterium *Pseudomonas elodea*. Glucose units in gellan are partly acetylated, which makes the molecule soluble. After chemical deacetylation, gellan forms strong gels, but otherwise, only weak gels are formed [37]. One of the applications of gellan is in the food industry as a thickener, stabilizer, emulsifying and gelling agent. It is also used as a medium for the growth of bacterial cultures [42]. There are, however, wide possible applications of gellan in pharmacy and medicine. It can be used in tablets as a matrix forming excipient for sustained release, or in in situ gelling systems as thickening and gelling agent. In tissue engineering, gellan may be used as an injectable carrier for cells or as a component of wound dressings [43].

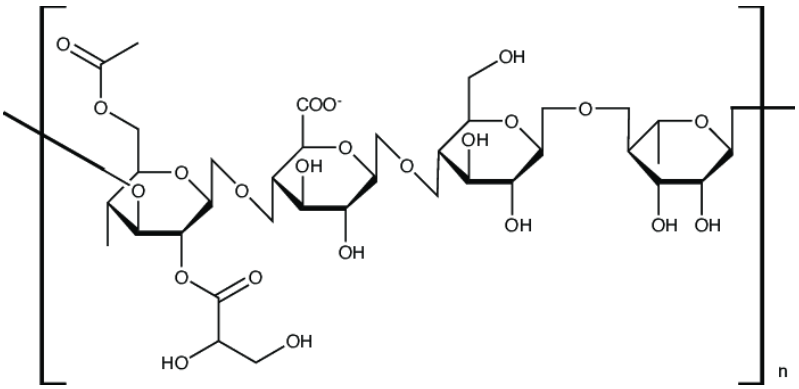

Figure 9 Chemical structure of gellan [44]

3 STATE OF THE ART

As the experimental part of this thesis is focused on the use of microrheological methods on hydrogels, the aim of this part was to review papers published on this topic. Specifically, the use of various microrheological methods to characterise colloidal dispersions, especially hydrogels, and the comparison of obtained data to bulk rheology. Although macro and microrheology focus on the same problematics, they use a completely different approach, which is why comparing the information obtained by those different methods can be a difficult task.

Guigas et al. [45] have used FCS as a passive microrheological method in their study of viscoelasticity of cytoplasm and nucleus in living cells. Fluorescently tagged inert gold beads with the diameter of 5 nm were used as the microrheological probe. Complex shear modulus of the fluids was obtained from the measured MSD by Laplace transformation. Both cytoplasm and nucleoplasm show non-Newtonian behaviour. At frequencies below 1 Hz, viscous modulus dominated in both cytoplasm and nucleoplasm, while at higher frequencies, the elastic portion arises and G´ and G´´ are of the same order of magnitude. Authors conclude that FCS is a convenient tool for the characterization of complex viscoelastic fluids even within living cells or tissues.

FCS was also used to probe local rheological properties of high molecular weight poly(ethylene oxide) solution by Rathgeber et al. [46]. Results from FCS were compared to macrorheology, and the same frequency dependence of viscoelastic moduli was observed, although the absolute values differed for 5% solution. Authors highlight the possibility to use probes with nanoscale diameters and spatial resolution as main advantages of FCS over other microrheological methods. In this study, fluorescent polystyrene tracer particles with diameter of 100 nm were used.

Krajina et al. [47] used DLS to study viscoelasticity of polymer gels (chemically crosslinked polyacrylamide (PAA)) and biological materials (linear DNA, extracellular matrices, intestinal mucus). Probe particles with the diameter of 100 nm were used. For the PAA gels, authors found that the value of the complex modulus is underestimated by almost a factor of 2 in DLS experiments compared to macrorheology in stiffer (5% and 10%) gels. That could be due to more inhomogeneities in those samples formed during rapid polymerization. In softer, less concentrated gels, a good agreement between the two methods was found. For biological samples, only DLS was used because of the limited amount available. Authors highlight the broad range of frequencies as one of the main advantages of DLS microrheology – up to 10^6 Hz, compared to 10^2 Hz in oscillatory rheology. For biological samples, often precious and costly, the significantly smaller volume that is needed for measurements (12 μl in this work) is another benefit.

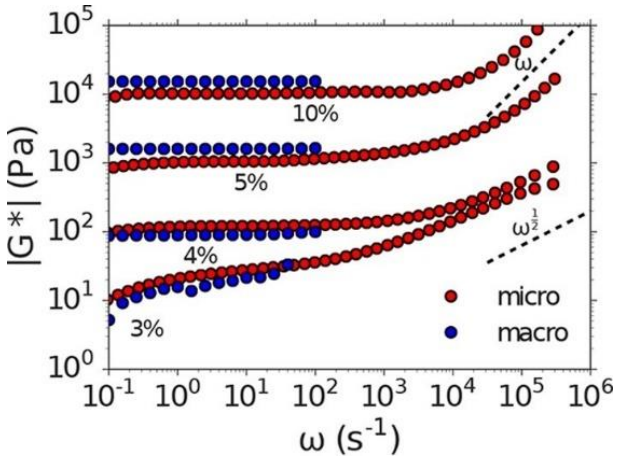

Figure 10 Comparison of G of PAA gels obtained by micro (DLS) and macrorheology [47]*

Cai et al. [20] later elaborated on this work and the use of DLS in microrheology. They used various classes of soft materials (hyaluronic acid solution, polyethylene glycol gels, hyaluronic acid gels) with different probes to explore the range in which DLS can be used. Hyaluronic acid solution was used as an example of polymer solution with polystyrene particles of two different diameters – 100 and 2000 nm – to study the effect of sedimentation during measurements. Authors conclude that with small particles like the ones with diameter of 100 nm, sedimentation does not play a role. Another class of materials explored are covalently linked polymer gels. Polyethylene glycol gels were used as an example and 500 nm polystyrene particles were used as probes. Here, authors highlight the importance of careful selection of the surface chemistry of the probes and their proper distribution before gelation. Gelation kinetics were examined, and it was determined that the system takes around 16 hours to reach equilibrium gel state. Hyaluronic acid gels were used as an example of material with physical bonding, and was probed with golden nanoparticles with diameter of 30 nm. Lastly, cancer cells embedded in extracellular matrix were studied to show the possibility of using DLS to study active biological processes.

In this work, authors also discuss advantages and limitations of DLS that have been mentioned previously. Apart from that, they propose future directions for DLS microrheology, such as implementing 96-well plates for higher-throughput capacity and automated measurements of several samples. Another prospect could be integrating DLS with a microscopic method to enable spatial resolution and provide additional information [20].

The suitability of microrheology for examining biological samples is stressed by Weihs at al. [48]. In their article, they focus on the field of bio-microrheology, studying mechanical properties of living cells.

Oppong et al. [49] studied a hydrogel made of polymer Carbopol by DLS, PTM and macrorheology. The aim of this study was to compare those methods and explore differences between macro and microscopic properties. Polystyrene latex spheres with the diameter of 0.49 μm and with a fluorescent dye were used as the probe. MSD obtained from DLS and PTM were in good agreement. Data from particle tracking show inhomogeneities in the gels, as the distribution of particle trajectories is not gaussian as is expected for Brownian diffusion. Viscous and elastic moduli obtained by bulk rheology are significantly larger (by orders of magnitude) than those obtained by DLS and PTM. The results are represented in Figure 11. The symbols represent data from rheometry (solid symbols G´, open symbols G´´)

for different concentrations of samples, lines showing results from microrheology (heavy lines G′, light lines G′′). That also shows the heterogeneity of the gel which is probed by individual particles but not by macroscopic measurement.

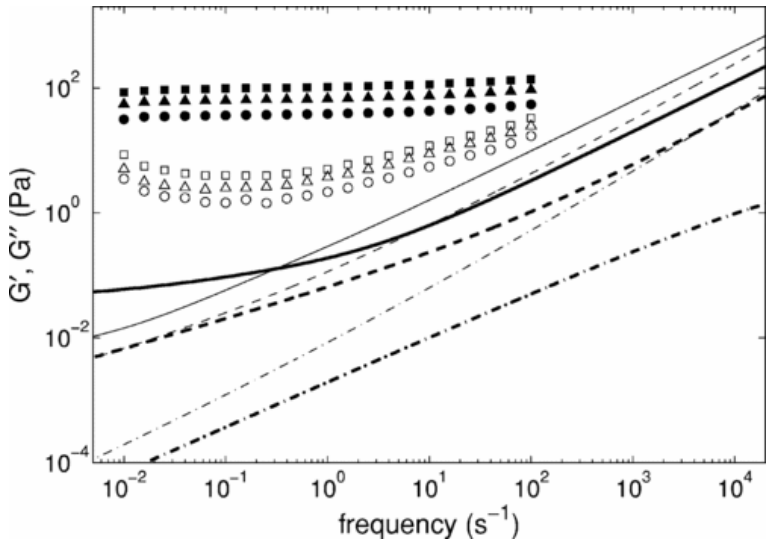

Figure 11 Viscoelastic moduli as a function of frequency, obtained by rheometry, PTM and DLS microrheology [49]

Optical tweezers were used as a microrheological tool by Tassieri et al. to measure the viscosity of water and polyacrylamide (PAM) solutions [50]. First, they measure the thermal fluctuations of a trapped bead, and secondly the displacement of the bead as a result of a uniform fluid flow. Particles with the diameter of 5 μm were used, and the data analysis was done with Labview particle tracking software. The optical trap stiffness was determined to be 0.8 μN/m in water and 1.7 μN/m in PAM 0.5% and 1% solutions. In the case of water, a constant viscosity was measured over five frequency decades. PAM solution, on the other hand, showed non-Newtonian behaviour, and the results are shown in Figure 12. The results were smoothed to remove experimental noise.

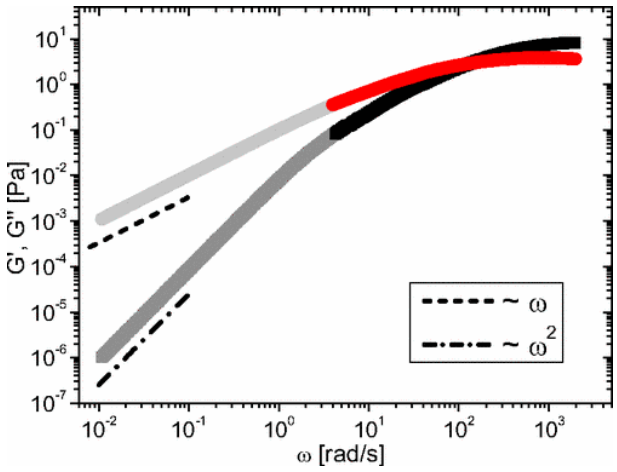

Figure 12 Storage (dark grey/black) and loss (light grey/red) moduli of a 1% PAM solution on water [50]

The team around the same author later published a work focused on data analysis procedure of microrheology with OT [29]. They used a titanium-sapphire laser to trap silica particles with 2 and 5 μm diameter. Samples were placed on a motorized microscope stage. A

LabVIEW particle tracking software was used to process obtained images. Solutions of actin filaments were studied and their viscoelastic moduli were obtained.

Pesce et al. used OT microrheology to measure viscoelastic properties of hyaluronic acid (HA) solutions and compared obtained results with macrorheology [51]. Rheological properties of solutions at concentrations ranging from 0.1 to 30 mg/ml were investigated. Polystyrene particles with diameter of 1.25 μm were used as the probe, a diode laser emitting at the wavelength of 830 nm was used for trapping and a photodiode was used as the sensor to record displacements of the probe. Authors found that the results from OT agree with the results from rheometry, which can be seen in Figure 13.

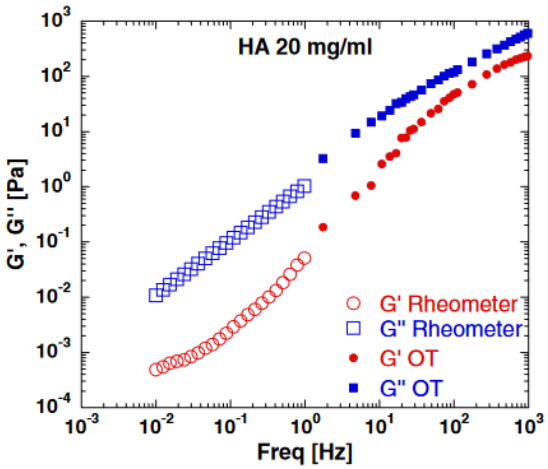

Figure 13 Viscoelastic moduli of 20 mg/ml HA solution obtained by OT (solid symbols) and rheometry (open symbols) [51]

Another work on the topic of OT microrheology was done by Brau et al. [30]. The complex shear modulus of complex fluids and polymer solutions was determined with both passive and active approach. Stiffness of the optical trap was calibrated in each sample with the equipartition theorem, and viscosity was determined with the Stokes drag method, monitoring the displacement of the trapped bead under external fluid flow. Glass beads of the size 490 nm were used. First, viscosity of solutions of glycerol with water was measured and compared to known data to validate the method. Then, time-dependent behaviour of methylcellulose solutions and actin networks was determined. Two different concentrations of actin were used, 1 μM and 10 μM and the measured viscoelastic moduli are shown in Figure 14.

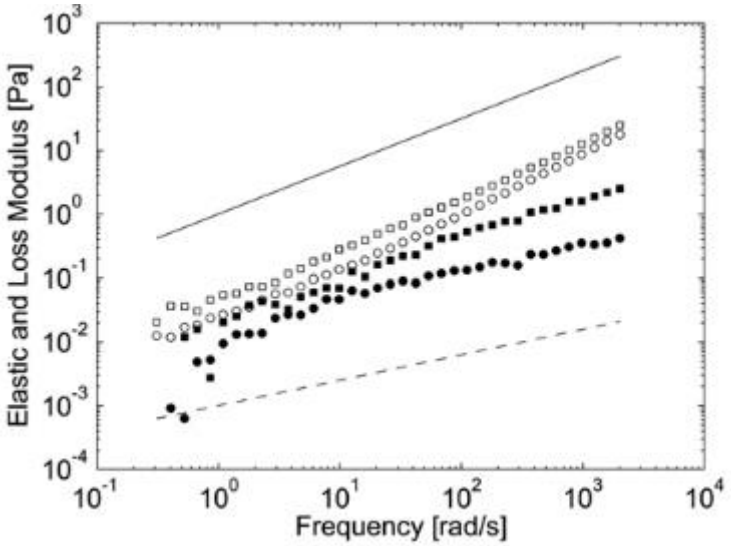

Figure 14 Storage (solid) and loss (open) moduli of action solutions of concentrations 1 M (circles) and 10 M (squares), measured by OT passive microrheology [30]

Active microrheological approaches were also introduced. One way to exert active force onto the sample is by displacing the optical trap location in a sinusoidal force function, monitoring its position and the position of the bead. From the phase angle difference between the force and the bead response, elastic and viscous moduli can be determined. Another way is to abruptly displace the trap away from the particle, which is then pulled to a new equilibrium position [30].

Microrheology at Faculty of Chemistry VUT

Microrheology is by far not a new topic at Faculty of Chemistry, and it has already been studied in various theses.

First example is the dissertation of Zuzana Hnyluchová [52], in which she studied passive microrheological techniques, concretely PTM, DLS and FCS. She studied glycerol solutions and hyaluronic acid (HA) solutions with all of those methods and found good agreement between them and also macrorheology. DLS was also used to study temperature dependent behaviour of hyaluronan solutions and for gelation of agarose, because a precise thermostat is a part of the instrument and so it is the most suitable method for measuring temperature dependant behaviour. In hyaluronan solutions, viscosity measured by DLS was distinctively different from the values obtained by rheometry. That means that temperature has bigger influence on macrostructure than it has on microstructure. HA gels are not transparent, therefore only video tracking microrheology could be used for their characterization.

Another dissertation on the topic of microrheology was written by Jakub Mondek [53]. He compared FCS with DLS and PTM, glycerol and HA solutions were used as materials. Newtonian fluids (water and glycerol) yield the same results in both DLS and FCS. Non-Newtonian hyaluronan solutions, however, show different results, and the deviation is larger with higher molecular weights of hyaluronan. This can be caused by interference of the polymer chains in DLS, as the light scattering is non-specific and the polymer chains also contribute to the scattering intensity fluctuations. The author estimates FCS as a more suitable method for viscoelastic materials than DLS.

Microrheology of hydrogels was a topic of the diploma thesis written by Denisa Píšová [54]. DLS microrheology was optimised on agarose hydrogels, and gels with the addition of polyelectrolytes were studied. The optimalization of DLS microrheology resulted in parameters that were used for the experiments in this work. Polystyrene particles with the size 100 nm were used in the ratio 40 μl of particles per 10 ml of sample. The position of measurements was 1 mm from the side of the cuvette. In this work, agarose gels of concentrations from 0.01 to 1 % were studied and 0.5 % gel was selected as the optimal concentration for further experiments with the addition of polyelectrolytes.

Another diploma thesis on the topic of microrheology was written by Petra Kábrtová [55]. The technique used in this thesis was FCS and it for used for the characterisation of hyaluronate-cetyltrimethylammonium bromide hydrogels. Fluorescent particles of sizes 30 and 300 nm were used. The author concludes using particles bigger than 100 nm to be unsuitable for the characterisation and 30 nm particles were used further. Laser of the wavelength of 470 nm was used for excitation and emission filter of wavelength 520/35 nm for the confocal detection. First, hyaluronic acid (HA) solutions, and then hydrogels were studied. In comparison of those measurements, the author concludes that measurements of hydrogels are more difficult in the sense of preparation, measurement itself and data analysis. Despite that, she highlights the potential of FCS microrheology, particularly for its sensitivity.

4 EXPERIMENTAL PART

4.1 Chemicals

- Agarose, low EEO, Sigma Aldrich, A6013-50G
- Phytagel, Sigma Aldrich, P8169-250G
- Glycerol, Sigma Aldrich, G9012-1L
- Milli-Q water

Particles:

- Micro particle size standard based on polystyrene monodisperse, size 0.1 μm, Sigma Aldrich, 90517-10ML-F
- Micro particles based on polystyrene, size 1 μm, Sigma Aldrich, 89904-5ML-F
- Sicastar®-greenF; green fluorescent silica particles with plain surface, size 50 nm; Product code:42-00-501

4.2 Instruments

- Zetasizer Nano ZS, Malvern
- Time-resolved Fluorescence Microscope *MicroTime 200*, PicoQuant
- Optical microscope *NIKON Eclipse Ci* with Laser diode driver, Mainman Electronics and ITS camera
- Rheometer *Discovery HR-2*, TA Instruments
    - Crosshatched plate, diameter 20 mm, serial number 115802
- Analytical scales 224A, Denver instruments
- Water purification system, Purelab Classic 091083-GBR-001

4.3 Software

- Zetasizer software
- SymPhoTime 64
- Matlab
- TRIOS
- Excel
- Origin
- TA Data analysis

4.4 Preparation of samples

4.4.1 Dynamic light scattering

Agarose gels for DLS measurements were prepared by mixing the necessary amount of agarose into 10 ml of Milli-Q water to reach the desired concentration (0.05 g of agarose for 0.5% gel etc.). 100 μl of polystyrene particles, size 0.1 μm, were added. The beaker was sealed to prevent evaporation and the mixture was heated to 85 °C in a water bath with constant stirring to completely dissolve the agarose powder. Approximately 1 ml of the sol was transferred to a glass cuvette. Measurements were done after 15 minutes, after the gel cooled down to laboratory temperature.

To test the effect of the concentration of particles on the quality of the results, samples with 40 and 150 μl of particles per 10 ml of the sample were prepared. The concentration of particles must be high enough to provide sufficient signal. If it is too high, though, unwanted effects like multi scattering or turbidity can occur.

To determine the effect of the manner of sample preparation on the results, some samples were submerged into the ultrasound heated to 60 °C directly after dissolving the agarose powder. This was done to ensure that no air bubbles would remain in the samples and cause experimental noise.

Gellan gels were prepared in a nearly identical manner as agarose hydrogels, the only major difference was in heating the samples to 90 °C to properly dissolve the Phytagel powder.

4.4.2 Fluorescence correlation spectroscopy

Agarose and gellan gels were prepared in the same way as for DLS measurements, but with different microrheological particles. Green fluorescent particles, size 50 nm, were used. First, the particles were diluted by adding 100 μl of the particles to 20 ml of water. From this solution, 30 μl was transferred onto the cover slide place in a holder. 1 ml of hot agarose/gellan sol was transferred onto the cover slide and mixed with the particles. Measurements were done after the samples cooled down to laboratory temperature and gelled.

4.4.3 Optical tweezers

A diluted solution of PS particles, size 1 μm, was prepared by adding 10 μl of the particles in 50 ml of water. Samples (water and glycerol solutions) were prepared by mixing 1 ml of the diluted particle solution with 3 ml of either water or glycerol. It is crucial to ensure that only one particle is trapped at a time for a proper measurement, which is the reason for the significant dilution.

20 μl of the sample was dropped onto the glass slide and covered with the cover slide. The glass slide was secured in the holder to limit any unwanted movement.

4.4.4 Rheometry

All samples for macrorheological measurements were prepared in the same way as for the other methods, without the addition of microrheological particles. 10 ml of each gel was prepared and measurements were done the next day after sample preparation.

4.5 Measurements and data evaluation

4.5.1 Dynamic light scattering

Measurements were done on Zetasizer Nano ZS in a measuring module Microrheology. Zetasizer software was used for data analysis. The software calculates mean-square displacement (MSD) curves as well as viscoelastic moduli from the measured autocorrelation function.

Measuring position was 1 mm from the cuvette wall, based on the calibration measurements done in the diploma thesis by Denisa Píšová [54]. Selected measuring position should minimise multi scattering. Each sample was measured 3 times. Equilibration time for temperature adjustment was 120 s for 25 °C.

For the measurements of gelation, the sample was first heated to 85 °C, the temperature was then reduced by 10 °C at a time and the sample was measured 3 times after each temperature reduction. The equilibration time was 15 minutes after heating to 85 °C and 5 minutes after each reduction of temperature.

The outcome of a DLS measurement is the correlation function, from which the MSD and viscoelastic moduli are calculated. An example correlation function, measured for 100 nm particles dispersed in water, is presented in Figure 15.

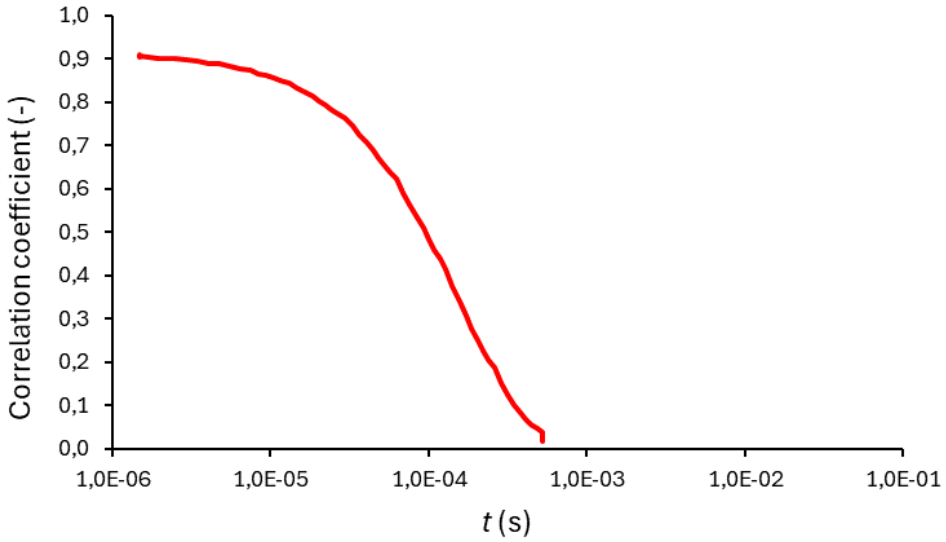

Figure 15 Correlation function for 100 nm particles in water

4.5.2 Fluorescence correlation spectroscopy

Time resolved fluorescence microscope Microtime 200 was used for FCS measurements. Measured data were analysed in software *SymPhoTime 64*. *Matlab* was used to obtain MSD curve from the autocorrelation function.

Before the microrheological measurements, a calibration of the microscope was done using a fluorescent probe Atto 88. From the calibration, characteristic values for the confocal volume were obtained, namely the effective volume V_{eff} and κ, characterising the ratio of height and width of the confocal volume. These characteristics are crucial in the fitting of the autocorrelation function.

The output of an FCS measurement is the time-dependant autocorrelation function $G(t)$. A model is fitted to the raw data, in this case it was the model for pure diffusion. Through a script in *Matlab*, the autocorrelation function is converted to a MSD curve by expressing it as a cubic equation from equation 18. If MSD is the variable x, $\langle r^2(t)\rangle = x$, the equation can be written as [55]:

$$\frac{2}{3w_{xy}^4 w_z^2}x^3 + \left(\frac{2}{w_{xy}^2 w_z^2} + \frac{4}{9w_{xy}^4}\right)x^2 + \left(\frac{4}{3w_{xy}^2} + \frac{3}{2w_z^0}\right)x + 1 - \frac{1}{N^2\left(G(t)\right)^2} = 0 \qquad (22)$$

w_{xy} and w_z are the dimensions of the confocal volume, N is the number of fluorescent particles in the confocal volume, and $G(t)$ is the autocorrelation function.

From the MSD, the creep compliance J is calculated through the following equation:

$$J = \frac{3\pi r}{dk_B T}, \qquad (23)$$

where r is the radius of the particles used, d is the number of dimensions in which the motion happens, k_B is Boltzmann constant, and T is temperature.

In *TA Data analysis* software, J is converted to viscoelastic moduli or complex viscosity. First, J values are plotted and a rheological model for discrete retardation spectrum is fitted based on equation 24:

$$J(t) = J_g + \frac{t}{\eta_0} + \sum J_i \cdot \left(1 - e^{(-t/\tau_i)}\right) \qquad (24)$$

η_0 is zero shear viscosity, J_g is instantaneous compliance and J_i are partial compliances corresponding to viscoelastic relaxation times τ_i. The retardation spectrum is transformed to the discrete relaxation spectrum and then to the frequency dependence of viscoelastic moduli or complex viscosity.

4.5.3 Optical tweezers

OT measurements were done with optical microscope Nikon Eclipse Ci with oil immersion objective, ITS camera and laser diode driver from Mainman electronics. Videos were taken in *Eye Cockpit-UI 324 x CP* in .avi formate. Camera settings were adjusted to maximise the frame rate and achieve more accurate results. By adjusting the microscope to provide maximal brightness, lowering exposure time to 200 μs and lowering the size of the cutout of the video to 140·140 pixels, frame rate of 155 Hz was reached.

Using a calibration grid, the size of one pixel was determined to be 66.8 nm. This value was used to calculate deflections of the particles from their positions.

Videos were analysed by a script in *Matlab* provided by the Institute of Scientific Instruments of the Czech Academy of Sciences. From the video file, position of the particle at every frame is detected. Visualisation of this step is shown in Figure 16. Knowing the size of each pixel from the calibration, displacement x [m] of the particle from its equilibrium position can be counted at each frame. The displacements are in the scale of nanometres to tens of nanometres, which means they occur on a sub-pixel level, so a correlation-based algorithm is used to determine the precise positions by comparing each image to a template. Obtained data were plotted in *Origin*.

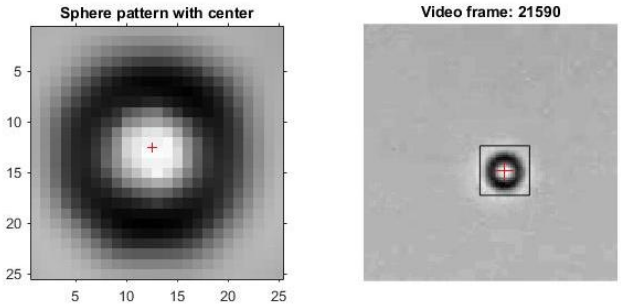

Figure 16 Visual analysis of data from OT

From the displacements from the trap centre, the optical trap stiffness κ was calculated using following equation, where $\langle x^2 \rangle$ is the average displacement of the bead over the measured time period, k_B is the Boltzmann constant, and T is temperature:

$$\frac{1}{2} k_B T = \frac{1}{2} \kappa \langle x^2 \rangle \tag{25}$$

4.5.4 Rheometry

Macrorheological measurements were done on the Discovery HR-2 rheometer with the plate/plate geometry with crosshatched surface and 20 mm diameter. Oscillatory tests were used to determine viscoelastic properties of samples, namely amplitude and frequency sweeps.

For amplitude sweeps, the frequency was held constant at the value of 1 Hz and the strain was changed from 0.01 to 1000 % in logarithmic mode with 6 points at each decade. For frequency sweeps, the value of strain was selected from the LVE region and frequency was changed from 0.01 to 100 Hz in logarithmic mode with 6 points at each decade. Before each measurement, the sample was kept at rest to relax and to adjust the temperature for 120 s for measurements at 25 °C and for 180 s for measurements at higher temperatures. Data were analysed in the *TRIOS* software and in *Excel*.

Although frequency of 100 Hz is theoretically reachable in the frequency sweeps, above 20 Hz, the results become unreliable because the samples can slip out of the measuring geometry. That can be solved by applying the time-temperature superposition (TTS) principle discussed in chapter 2.1.2. Frequency sweeps for TTS were measured at temperatures 5, 15, 25 and 35 °C and a master curve was plotted. By applying TTS, the frequency range was extended to 100 Hz.

5 RESULTS AND DISCUSSION

5.1 Dynamic light scattering

5.1.1 Gelation of agarose and gellan

Zetasizer enables precise temperature control during experiments, making DLS a suitable method for measuring temperature-behaviour of polymers. Agarose and gellan both form thermoreversible gels, and the gelation process can therefore be observed through DLS.

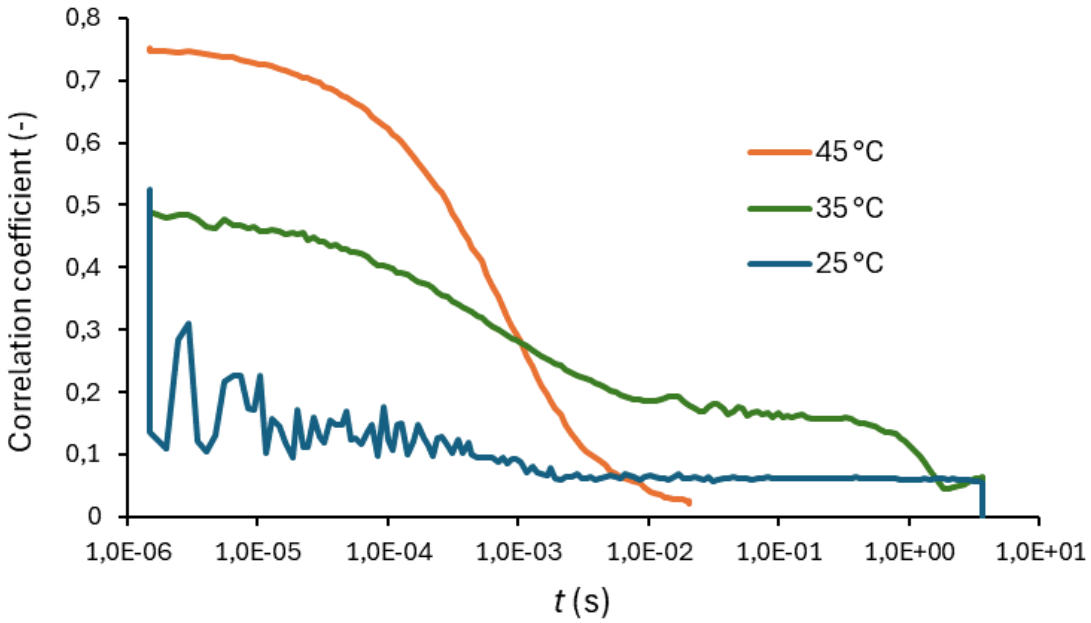

Figure 17 Correlation curves for 0.5% agarose at 45, 35 and 25 °C

Once the gel is cooled beneath its gelation temperature, which for agarose could be between 30 and 40 °C [40], the light starts to scatter from the gel structure as well as from the probe particles. The noise becomes significant, which is shown in the shape of the correlation curve (Figure 17). As the temperature lowers and the sol turns into a gel, the signal lowers as well. That is why results obtained at 25 °C need to be viewed and analysed with caution.

In the plot for 25 °C, the values of G′ and G′′ are quite scattered, which is another indicator of data of lower quality. Elastic modulus is prevalent, while at 45 °C it is inferior, implying that at 45 °C, agarose is still a sol. On the contrary, at higher frequencies, both moduli are larger at 45 °C. That is inconsistent with results from rheometry (Figure 19), which show that the viscoelastic moduli are larger at 25 °C, and even before gelation, at 45 °C, the elastic modulus still dominates over the viscous modulus. Those inconsistencies could be blamed on the shape of the correlation function at 25 °C, and therefore poor raw data. Another reason could lie in the different approaches of micro and macrorheology. As was found in studies mentioned in chapter 3 [47, 49], microrheology can underestimate the values of viscoelastic moduli, compared to macrorheology. Moreover, the microrheological approach can highlight the viscous portion of the complex modulus, because the probe only interacts with individual parts of the polymer network, while in macrorheology, the network is studied as a whole.

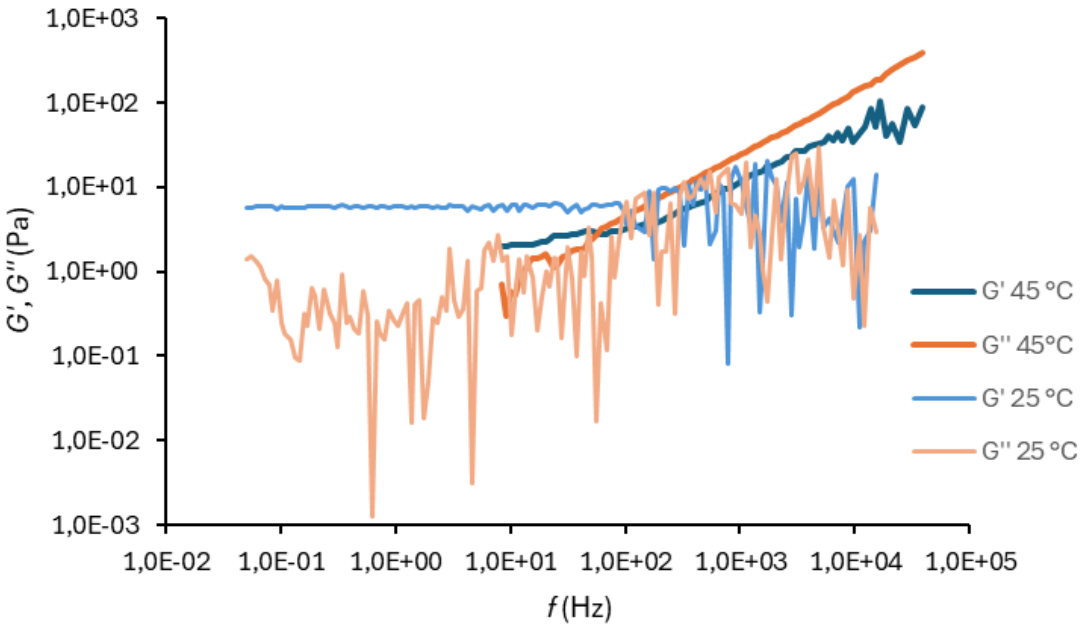

Figure 18 Viscoelastic moduli of 0.5% agarose from DLS at 45 and 25 °C

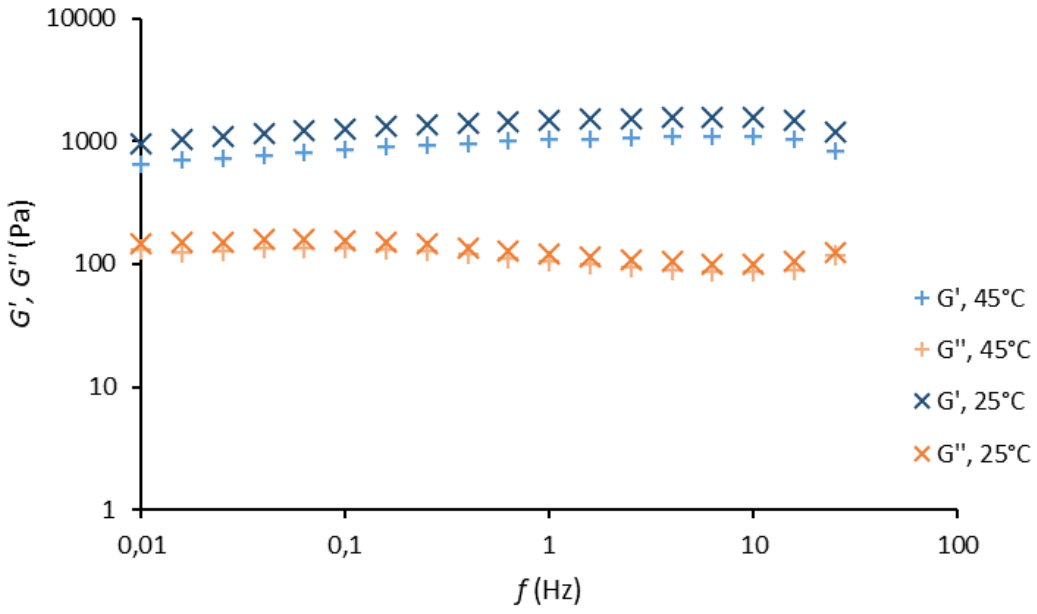

Figure 19 Viscoelastic moduli of 0.5% agarose from rheometry at 45 and 25 °C

Gelation experiments for 1% gellan show similar results to agarose. The calibration curve at 25 °C hints at some experimental noise, but indicates better raw data than for agarose. The viscoelastic moduli values are also less scattered. The overall results are, however, similar to those for agarose. At 25 °C, the elastic modulus dominates, while at 45 °C, it is the viscous modulus that prevails. Despite that, at higher frequencies, values of both G´ and G´´ at 45 °C surpass those obtained at 25 °C. This could show that even though the gel structure is not yet completely formed at 45 °C, some bonds are already forming and increasing the value of the complex modulus, although the viscous portion prevails.

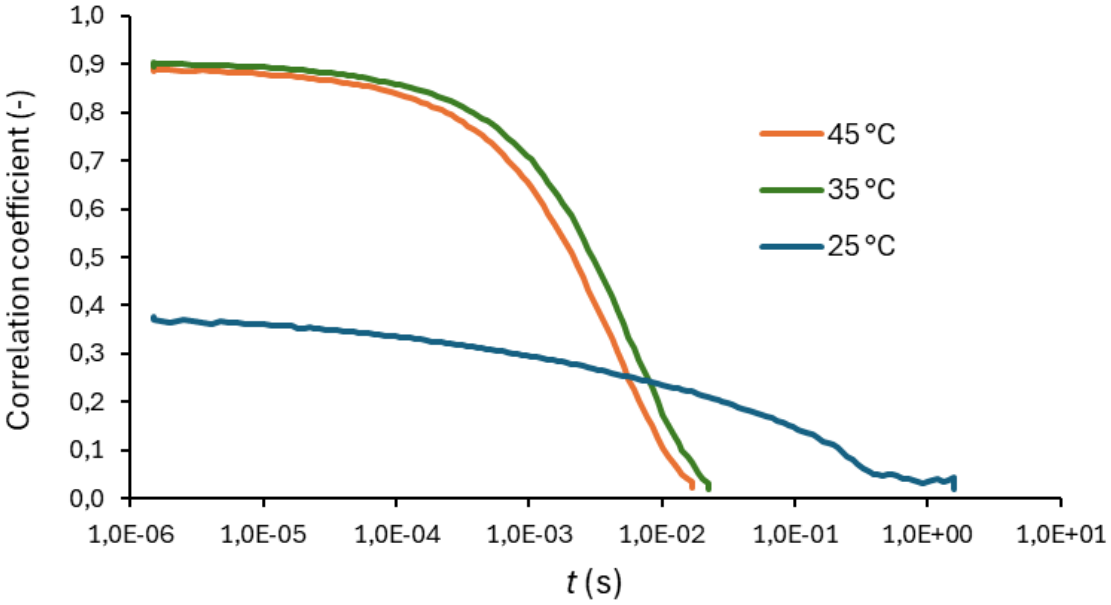

Figure 20 Correlation curves for 1% gellan at 45, 35 and 25 °C

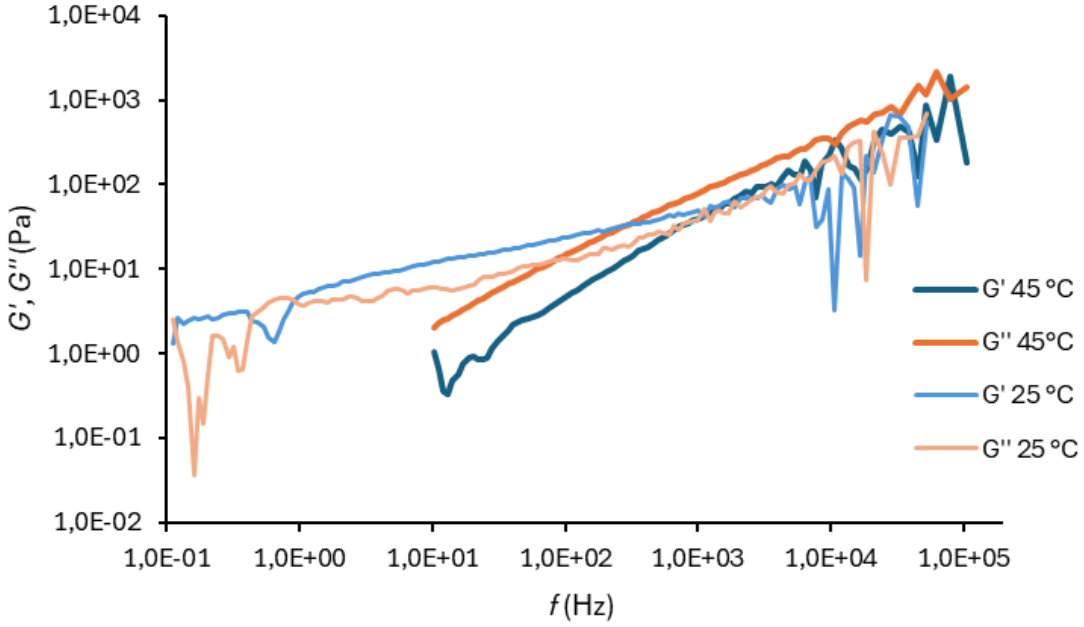

Figure 21 Viscoelastic moduli of 1% gellan from DLS at 45 and 25 °C

For both type of gels, the elastic modulus dominates at 25 °C, confirming that the hydrogel structure has already formed. Above 1000 Hz, the values become quite scattered for gellan gel, indicating some uncertainty of the validity of those values. This still means a significant extension of frequencies in regard to macrorheology, which will be discussed in the next chapter.

5.1.2 Comparison with macrorheology

With respect to the shape of the correlation curves, 1% gellan gel was chosen for the comparison with rheometry, specifically the measurement done at 35 °C. Gellan is a polymer similar to agarose, used as a substituent. It forms a weaker gel (based on the values of viscoelastic moduli obtained by rheometry) than agarose, and was possible to measure by DLS and obtain reliable data. Comparison of the autocorrelation functions obtained for 1% gellan and 0.5% agarose, both at 35 °C (Figure 22), shows the difference between the correlation curves.

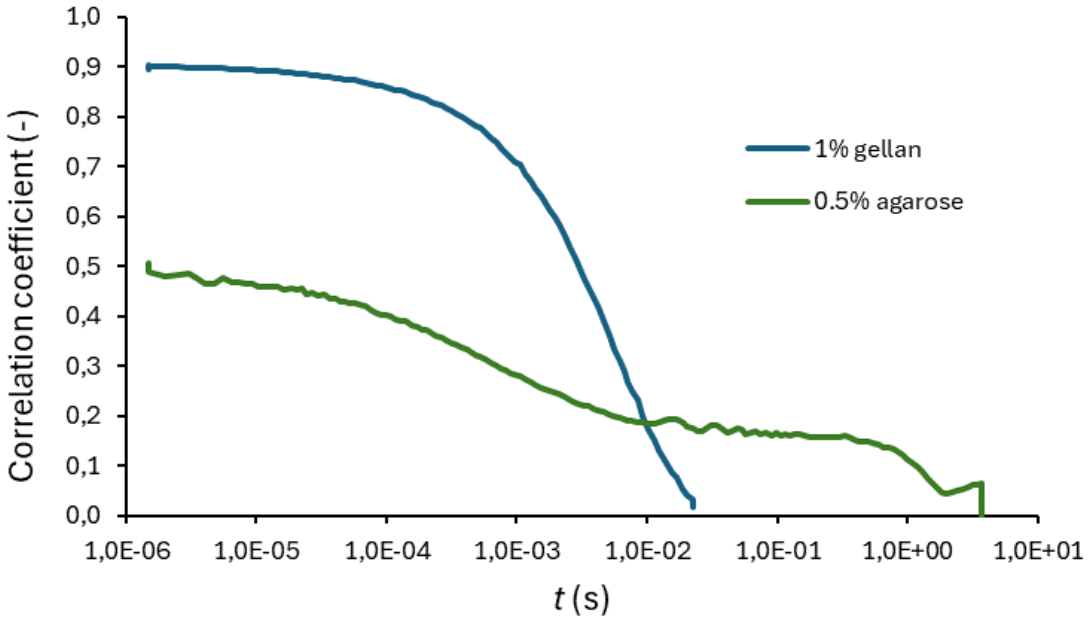

Figure 22 Correlation function for 1% gellan and 0.5% agarose at 35 °C

Macrorheological characterisation of 1% gellan gel confirms that it is a weaker gel than 0.5% agarose, with the elastic modulus higher than the viscous modulus, but with the values in the magnitude of only a 100 Pa. Theoretically, a rheometer can measure up to the frequency of 100 Hz, but since the values of G´ are so small, the results were quite unreliable from 20 Hz, when the "raw phase" data (phase shift between displacement and torque signal) suggest that the limits of the rheometer are reached. The data from DLS start at approximately 10 Hz and end at more than 10 000 Hz. That is why time-temperature superposition was implemented to prolong the range of frequencies from macrorheology and make it easier to compare the two methods.

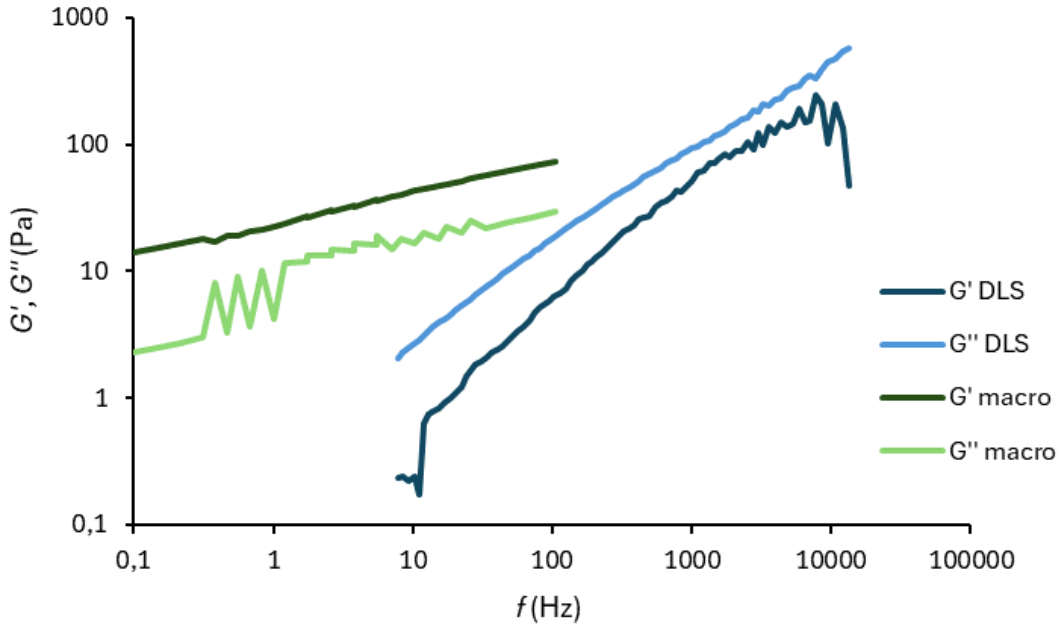

Figure 23 Comparison of DLS microrheology and rheometry for 1% gellan gel measured at 35 °C

First difference between DLS and rheometry is which modulus is dominant. As determined by rheometry, storage modulus is dominant. DLS measurement, on the other hand, shows the opposite, and the loss modulus is dominant in the whole frequency range. Another difference is in the values of both viscoelastic moduli, which, measured by DLS, are significantly smaller in the overlapping area. The trend in both methods is that both moduli rise with rising frequencies. Above 1000 Hz, values of G´ and G´´ from DLS exceed the values from rheometry. These frequencies far outreach the limits of rheometry, making it challenging to compare the results.

As for the agarose hydrogels, the results for 0.1% gel were chosen for the comparison with macrorheology. Rheometrical measurements of this gel reach the limits of the rheometer, same as for 1% gellan. That makes DLS a suitable complementary method to characterize the viscoelastic behaviour at higher frequencies. Values of G´ and G´´ obtained from DLS increase significantly and even surpass the values from rheometry at above 100 Hz.

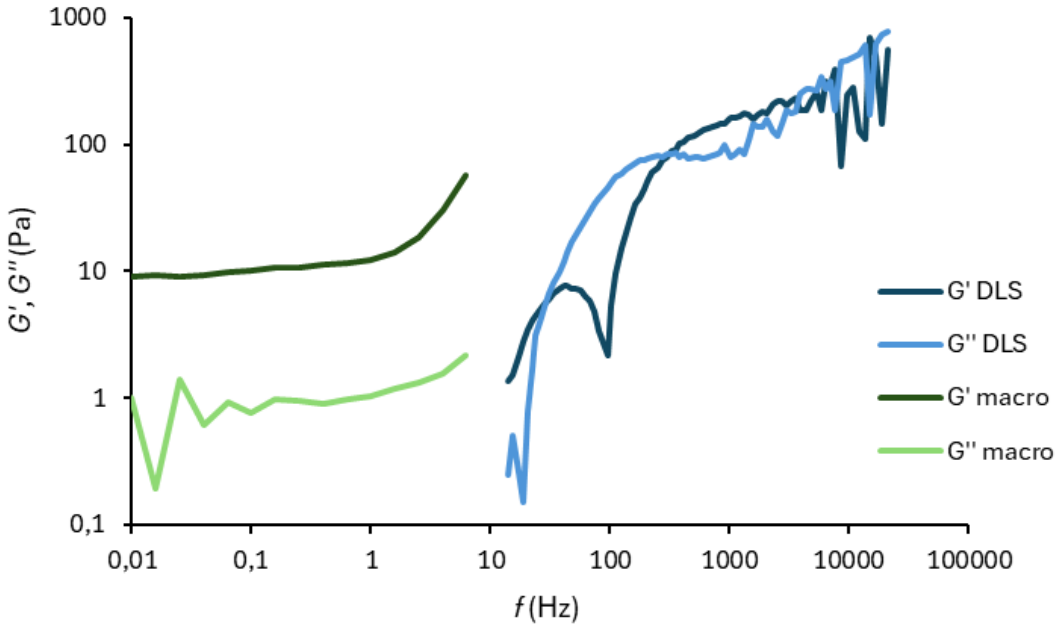

Figure 24 Comparison of DLS microrheology and rheometry for 0.1% agarose gel

Comparing DLS with macrorheology shows the advantages of the combination of those two methods. DLS can provide information about high-frequency viscoelastic behaviour, that is not possible to reach by oscillatory rheometry due to the limitations of the instrument.

5.2 Fluorescence correlation spectroscopy

Agarose gels of concentrations 0.1 %, 0.5 % and 1 %, and gellan gels of concentrations 1 % and 2 % were analysed by FCS. Before each measurement, a scan of the sample in the *x-y* axis was done, from which the places for measurements were chosen. On the images (Figure 25), places with visible clusters of particles can be seen. For measurements, places between visible clusters were chosen, because having only one particle in the confocal volume at a time is favourable for FCS experiments.

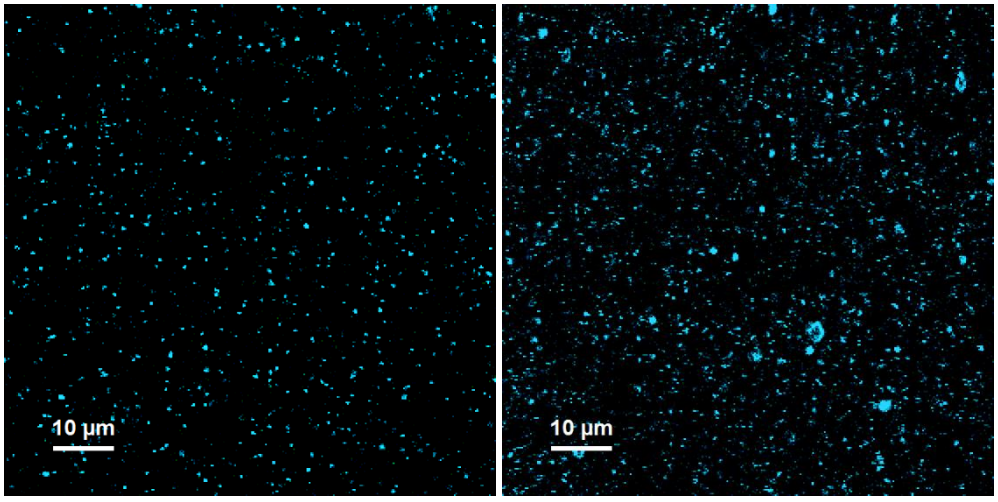

Figure 25 Images from FCS of 0.5% agarose (left) and 1% gellan (right) gels

A crucial quantity measured in microrheology is the mean square displacement. The MSD curves for all agarose concentrations are plotted against time in Figure 26. For 0.1% and 0.5% hydrogels, all three measurements gave almost identical results. For 1% agarose hydrogel, the curves vary, which indicates heterogeneities within the sample that do not occur in the less concentrated samples. Another reason could be that the path the particle undergoes is influenced more by a denser network, and therefore the MSD varies in the most concentrated gel and is almost the same for the less concentrated gels.

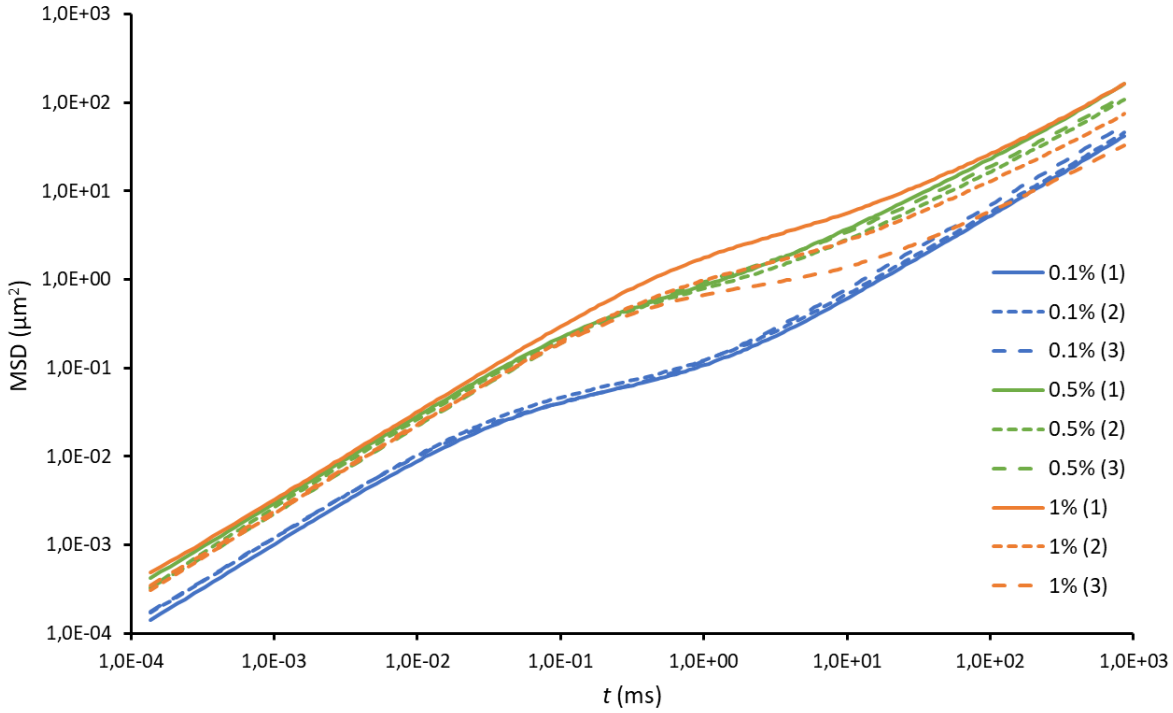

Figure 26 MSD curves for agarose hydrogels obtained from FCS

5.2.1 Viscoelastic properties of agarose and gellan hydrogels

From the MSD curves measured by FCS, viscoelastic moduli (complex modulus G^*, storage modulus G' and loss modulus G'') were calculated in *TA Data analysis* software by the procedure described in chapter 4.5.2. The final result is the frequency-dependence of storage and loss moduli. The representative result is for 1% agarose hydrogel (Figure 27).

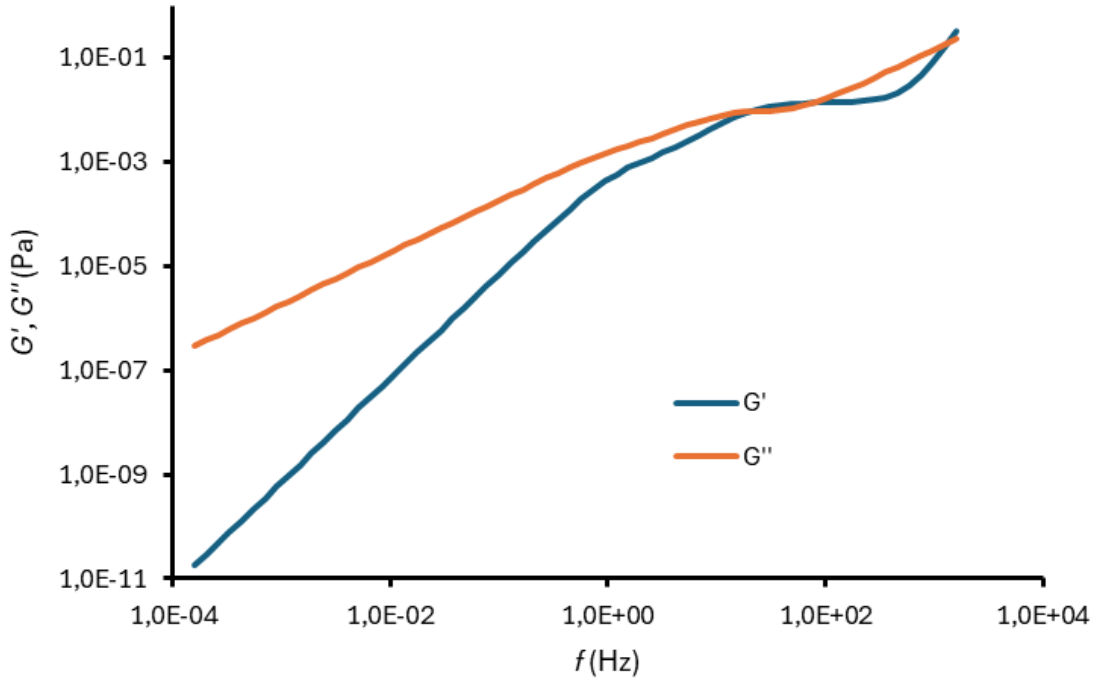

Figure 27 Storage and loss moduli of 1% agarose hydrogel

Values of both moduli increase with frequency until around 100 to 1000 Hz, where a plateau of *G'* values occurs. The viscous modulus is dominant in almost the entire frequency range. At around 100 Hz, the values of the elastic modulus briefly surpass those of the viscous modulus, but only for a short frequency period. That means that from the FCS microrheological point of view, the 1% agarose gel would be a viscoelastic liquid. The cause of this could be free diffusion of the microrheological probe through the gel network, which would mean that the chosen particles might be too small for this type of hydrogel.

Three different concentrations of agarose gels were measured. For the comparison between gels (Figure 28), the complex modulus was chosen for the simplification of the diagram. Results for gellan hydrogels, including the comparison of samples, were very similar and can be found in attachments.

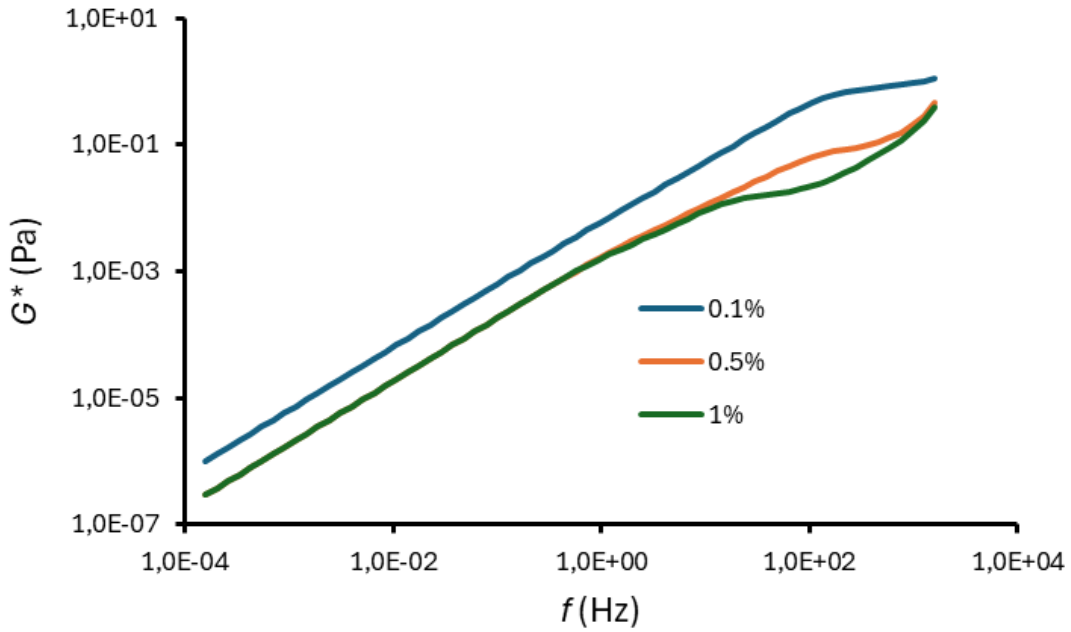

Figure 28 Comparison of complex modulus of different concentrations of agarose hydrogels measured by FCS

The results from FCS in Figure 28 are very similar for all agarose hydrogels, regardless of concentration. Rheometry, on the other hand, show significant difference in G´ and G´´ values (Figure 29). The reason could be an inadequate choice of probe size, which was 50 nm. If the microrheological is too small (smaller than the mesh size of probed sample), the results show properties of the solvent, not the hydrogel as a whole. Conclusion of a diploma thesis written on the topic of FCS microrheology [55] was that particles larger than 100 nm are too large and not suitable for hydrogel characterisation, because their diffusion is too slow. Results obtained for agarose hydrogels for this work suggest that the size of 50 nm might not be appropriate as well.

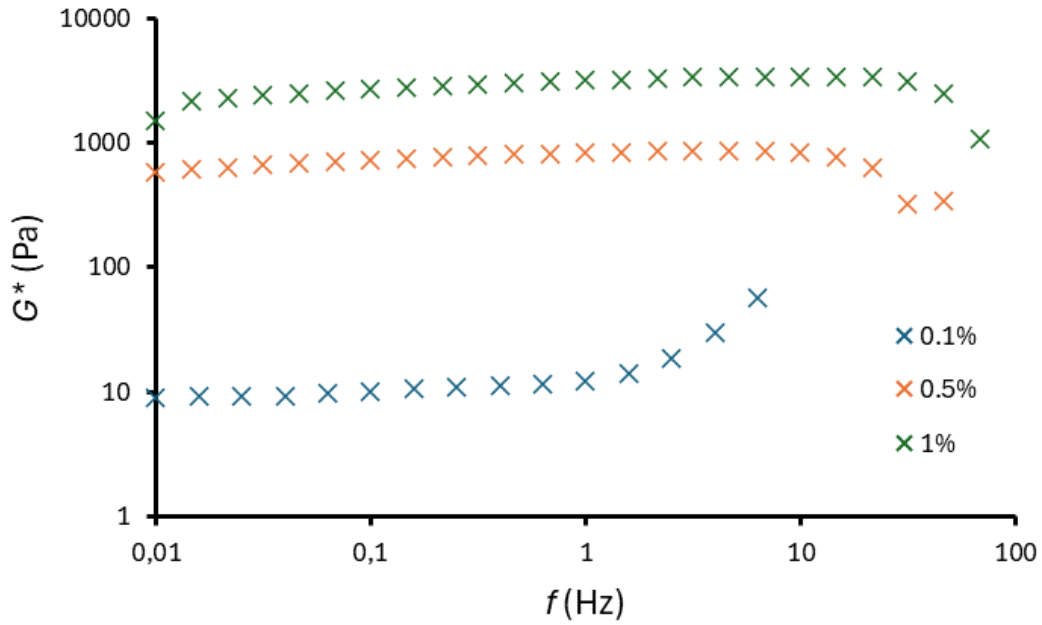

Figure 29 Comparison of complex moduli for agarose hydrogels obtained by rheometry

5.2.2 Comparison with macrorheology

Viscoelastic moduli obtained from the MSD measured by FCS were compared to those obtained by rheometry (macrorheology), namely oscillatory frequency sweeps.

In FCS measurements, significantly larger range of frequencies can be achieved. Rheometrical frequency sweeps can be measured from 0.01 Hz up to 100 Hz in theory, but in reality, only data up to 20 Hz are reliable. FCS on the other hand provides results from 0.0001 Hz to 1500 Hz.

A result for 1% gellan gel is in Figure 30. From the macrorheological point of view, the gel is a viscoelastic solid (storage modulus is greater than loss modulus) in the whole frequency range. FCS data suggests that the storage modulus becomes dominant in higher frequencies, but for lower frequencies, 1% gellan is a viscoelastic liquid.

FCS also underestimates the values of both G' and G'' by two orders of magnitude. That could cohere to the way the sample is viewed. The microrheological probe of the size 50 nm "sees" the microstructural elements of the sample, which could be much more compliant than the whole structure, "seen" by the rheometer. Similar results were found by Oppong et al. [49] when comparing DLS microrheology to rheometry. Nevertheless, both methods show the same trend of an increase in both moduli with increasing frequency.

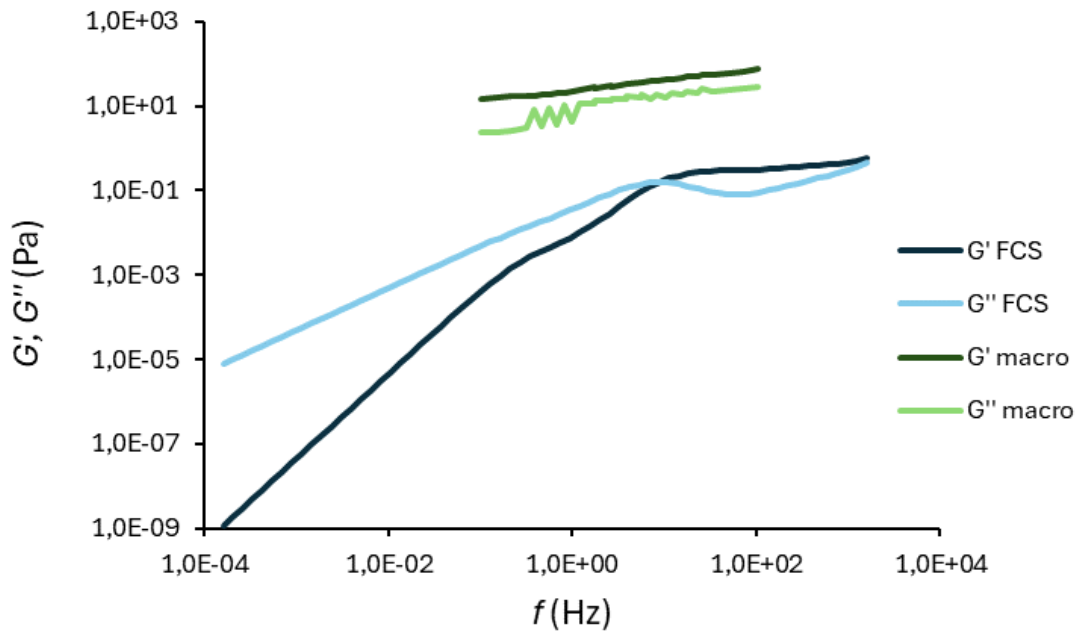

Figure 30 Comparison of viscoelastic moduli of 1% gellan gel obtained by FCS and macrorheology

5.3 Comparison of methods

DLS and FCS are, in some ways, similar methods. Both belong between passive microrheological methods, both record intensity fluctuations, from which correlation functions are formed. Their difference lies in the fluctuations that are recorded – scattered light from particles in DLS and excited fluorescence light from particles in FCS. The aim of this chapter was to show if they give comparable results when measuring viscoelastic properties.

From DLS measurements, 0.1% agarose and 1% gellan gave the best correlation curves. For that reason, those two samples were chosen for the comparison with FCS. First, MSD curves were compared (Figure 31).

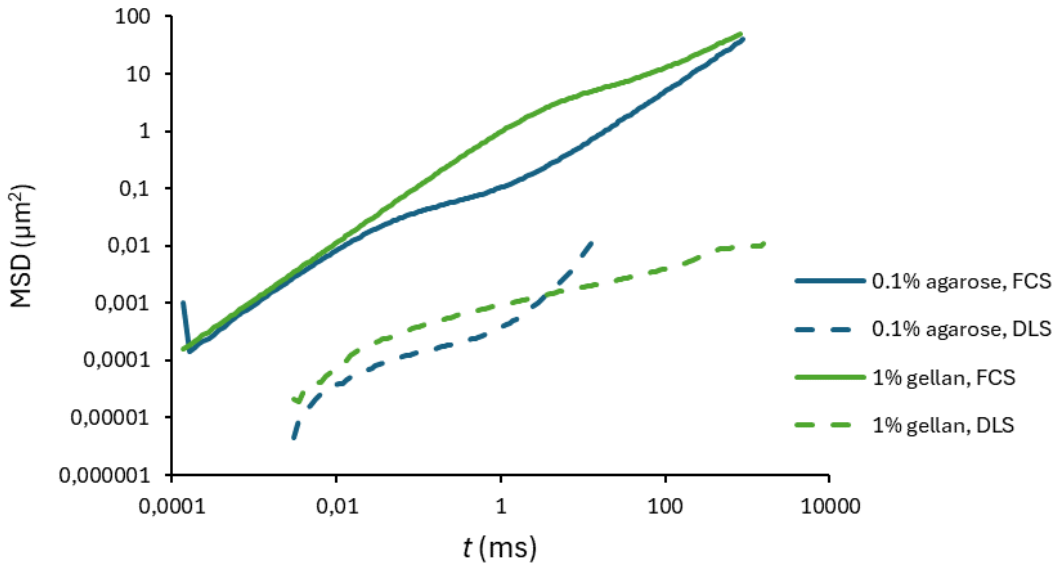

Figure 31 MSD of 0.1% agarose and 1% gellan from DLS and FCS

From recorded MSD, viscoelastic moduli are calculated. Comparison of results for agarose (Figure 32) shows that for both methods, G´´ is dominant at lower frequencies, but there is a cross point, indicating a slightly prevalent elastic behaviour at frequencies above 100 Hz.

For both samples, DLS gives higher values of both G´ and G´´, closer to those obtained by rheometry.

The frequency range is greater for FCS, however, DLS provides data even for frequencies above 10 000 Hz, which is not possible either by FCS or rheometry.

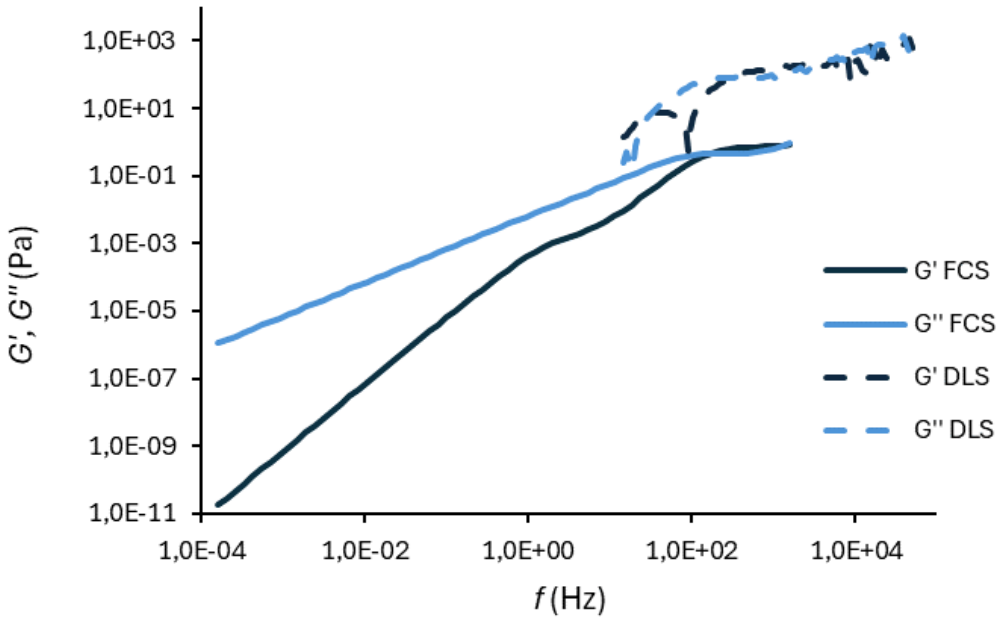

Figure 32 Viscoelastic moduli of 0.1% agarose from DLS and FCS

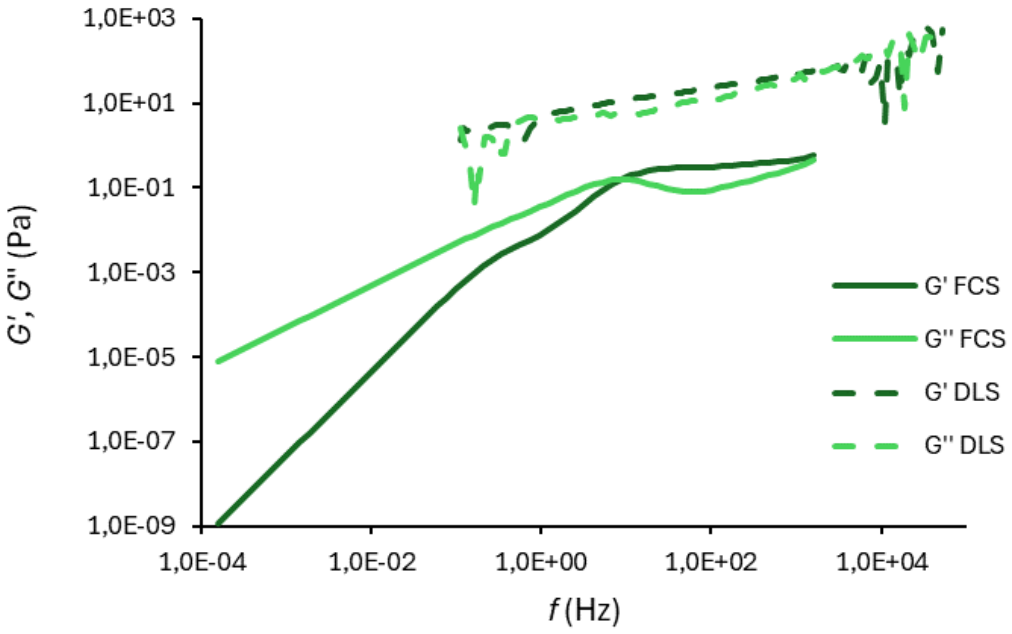

Figure 33 Viscoelastic moduli of 1% gellan from DLS and FCS

For both gellan and agarose, FCS and DLS are in a good agreement. Although the absolute values of both moduli are different, the plots are very much analogous. For agarose, the viscous modulus is dominant at low frequencies for both FCS and DLS, there is a crosspoint at almost the same frequency for both methods, and by the end of measurable frequency range, there is a hint of a second crosspoint. For gellan, the frequency range in which the elastic modulus is prevalent is broader, and again, this applies to both methods.

Comparison of DLS and FCS, both microrheological techniques, shows similarities between the measured data. The absolute values may differ, but otherwise, the course of the plotted data is analogous. The difference in absolute values could be due to the different size of the microrheological probes. Nevertheless, the conclusion of this comparison is that these two methods could substitute each other, based on the character of the sample and the applicability of each method.

5.4 Optical tweezers

Optical tweezers are a unique microrheological method. They rely on a similar principle as particle tracking microrheology – following Brownian motion of a particle. In OT, however, the tracked particle is weakly trapped by a laser beam and its motion consists of oscillation around the optical trap centre.

OT have not been previously used at the Faculty of chemistry, but they provide a different approach to microrheology measurements and an interesting view on the viscoelastic properties of samples.

5.4.1 Probe position analysis

After a particle was trapped by the laser, a video was taken and ran through the script for analysing the positions of the trapped bead at each frame.

A result of this analysis are deflections from the centre of the trap in time. Those deflections should be random and follow a Gaussian distribution, if the measurement is done right. Deflections against time and histograms were plotted to evaluate the validity.

Water and glycerol solutions have been measured so far. Data for water are shown in Figure 34 and Figure 35. Hydrogel systems have not yet been studied due to the ongoing calibration of experiments and lack of time.

In the time dependence of the bead position (Figure 34), any external effects on the measurement can be seen. The highest displacements are of 100 nm, which shows the extreme sensitivity of the method.

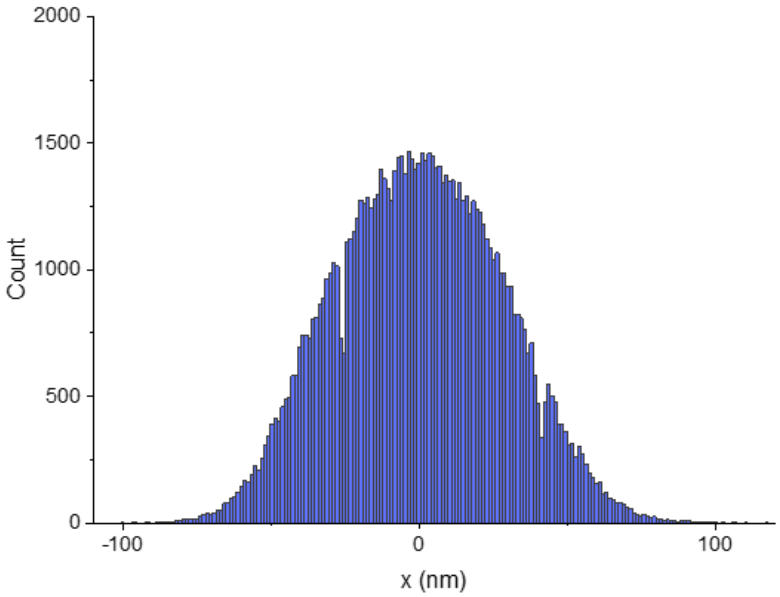

Figure 34 Histogram of deflections of a trapped probe in water

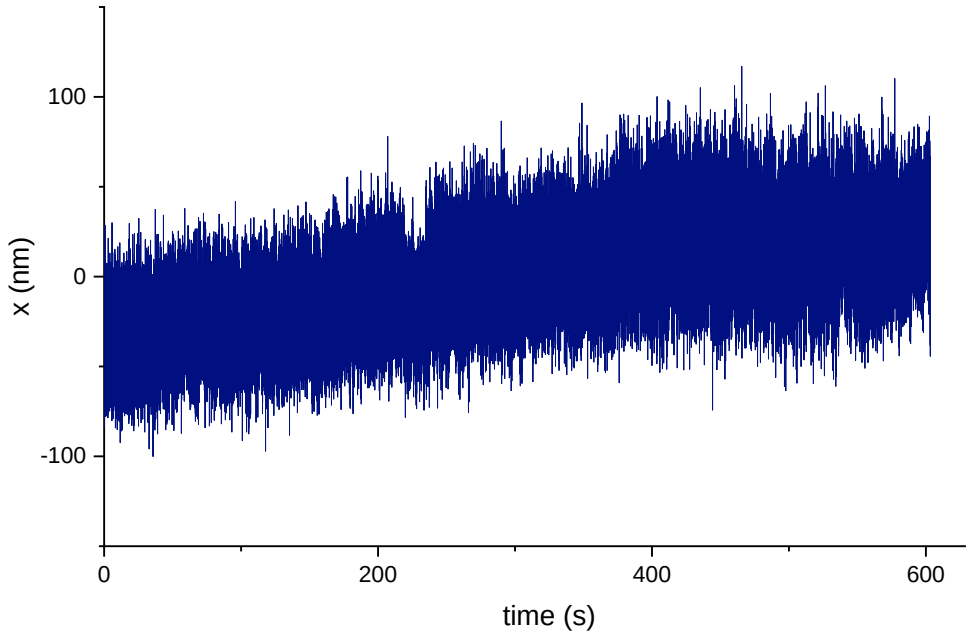

Figure 35 Time-dependence of the position of a trapped particle in water

5.4.2 Measuring the stiffness of the optical trap

Determining the stiffness of the optical trap in a sample is a crucial step in the characterisation of viscoelastic properties, as it calibrates the method to the measured sample. The trap can be imagined as a linear spring and its stiffness corresponds to the spring constant [30]. Stiffness is determined by measuring the displacements of a trapped particle from its position in the centre of the trap.

A suitable length of the video to provide reliable results needed to be specified. Authors in [29] say that the value of the stiffness should be determined from a *sufficiently long measurement*. The length of this measurement needed to be specified experimentally. A 10-minute-long video of a particle in water was taken. The optical trap stiffness was determined after each minute to find at which time it no longer changes. Results of this experiment are in Table 1. It was determined that a suitable length of videos for future measurements would be 8 minutes, because the value of κ continued to decrease only slightly in the last 2 minutes of the measurement.

Table 1 Values of optical trap stiffness

***t* (min)**	1	2	3	4	5
κ (N/m)	$1.26 \cdot 10^{-5}$	$1.23 \cdot 10^{-5}$	$1.12 \cdot 10^{-5}$	$9.88 \cdot 10^{-6}$	$8.34 \cdot 10^{-6}$
***t* (min)**	6	7	8	9	10
κ (N/m)	$7.45 \cdot 10^{-6}$	$6.23 \cdot 10^{-6}$	$5.56 \cdot 10^{-6}$	$5.36 \cdot 10^{-6}$	$5.27 \cdot 10^{-6}$

Measured optical trap stiffness in water is in the order of μN/m, which is consistent with the value determined by Tassieri et al. [50]. Each experimental setup is unique and requires its own calibration before measurements. Nevertheless, the consistency in the result confirms the validity of the experiment.

Next, the applicability of this method was tested. Glycerol was chosen as a liquid with a higher viscosity than water. The optical trap stiffness was measured in glycerol solutions with the concentrations of 25, 50 and 75 % v/v. The results are in Table 2.

Table 2 Optical trap stiffness in solutions of glycerol

Concentration	25 %	50 %	75 %
κ **(N/m)**	$4.02 \cdot 10^{-5}$	$4{,}56 \cdot 10^{-5}$	$4.11 \cdot 10^{-5}$

Optical trap stiffness measured for glycerol is greater than it is for water, with the same laser settings. That is also consistent with the study mentioned previously, where PAM solutions were measured, and κ had a greater value for those solutions than for water. Glycerol and PAM behave differently, but both are fluids of higher viscosity than water, so the comparison between those results is imperfect, but sufficient.

5.4.3 Future advances

Optical tweezers are a versatile method that can be used both for passive and active microrheology experiments [30]. Future proposals for experiments would be measuring the viscosity by monitoring the displacements of the trapped bed under constant flow of the surrounding fluid as was described in chapter 2.2.4.

Further development of the method would include acquiring MSD curves from the positions of the trapped bead. MSD can be converted to viscoelastic moduli, and OT could then be used not only for the characterisation of Newtonian fluids by obtaining their viscosity, but also for viscoelastic materials by determining their frequency dependent behaviour. Interpreting the elastic modulus by taking into account the elastic effect of the optical trap was also described in chapter 2.2.4.

6 CONCLUSIONS

The aim of this thesis was to pick microrheological methods suitable for hydrogel characterisation and compare them to macrorheological measurements. Dynamic light scattering, fluorescence correlation spectroscopy and optical tweezers were chosen as the microrheological tools. DLS and FCS are passive methods, while OT can be used for both passive and active microrheological measurements.

DLS and FCS are both well-established methods at the FCH and have been previously used as tools for microrheology at the Faculty of chemistry. OT are a new method, and optimalization of both experimental setup and evaluation of obtained data was needed. This was done in collaboration with the Institute of Scientific Instruments of the Academy of Sciences.

Microrheology offers a different view on the rheological properties of materials. Using a probe within the material allows a characterisation on a local level, which can show heterogeneities of the sample. Macrorheology, in the form of rheometry, remains a superior method for routine characterisation. It enables a rapid, simple and accurate characterisation of materials, ranging from liquids to viscoelastic solids. Microrheology usually requires a smaller volume of sample and is non-destructive, allowing for repeated measurements. That could mean an advantage over rheometry in the fields of biochemistry or medicine, where samples can be rare or expensive. The range of materials, that are possibly to study, is more limited. As the review of literature suggests, microrheology is suitable for complex (viscoelastic) liquids. Implementing these techniques to hydrogels can be complicated, as was found in the experimental part of this thesis. In a dense polymer network, the motion of the probe particle is significantly hindered and obtaining precise results requires careful optimisation of methods and preparation of samples. Another disadvantage of microrheology over rheometry is elaborate data analysis. A conventional rheometer provides comprehensible data even for a relatively inexperienced user. Microrheological methods used in this thesis require deeper understanding of the process, from the choice of probes to the understanding of the results and their validity. That being said, microrheology certainly deserves attention and has a future in the field of rheology.

Compared to macrorheological approach, DLS and FCS microrheology both underestimate the values of the viscoelastic moduli and emphasize the contribution of the viscous modulus. This provides an insight into the local structure of hydrogels. On the microscopic scale, the viscous modulus is more relevant than at the macroscopic scale, where the elasticity of the gel dominates.

The techniques used in this thesis each offer a different approach and benefits. DLS is a relatively simple method. The software provides both MSD and viscoelastic moduli counted from the autocorrelation function. It allows for measurements of temperature dependant processes and offers a wide range of frequencies. However, it requires a transparent sample, which is a significant limitation. It is also nonspecific, which means the polymer network in hydrogels can contribute to the scattered lights and compromise the results. This turned out to be a considerable issue in this thesis. FCS offers an advantage over DLS in its specificity. Using fluorescent probes limits the interference of the network and enables measurement of more elastic hydrogels. This also provides some limitations, like photobleaching of the probes or difficulty measuring fluorescent samples. Yet, based on the data provided in this thesis,

both methods can be used to characterise a sample and get comparable results. This means that the more suitable method for microrheological characterisation of a given sample can be chosen based solely on their advantages and limitations.

Moreover, only OT offers a different approach than the other two methods. One of the advantages of OT is the visual result, which allows control over the measurements. The data analysis is, however, demanding and requires knowledge of particle tracking algorithms and image processing. It is a very sensitive method, and the results can be disrupted by external impacts like talking, closing doors or people walking past the laboratory. The main limitation of this method for the purposes of this thesis was that it is a new and non-established method, so the applicability was limited. There are a lot of options to upgrade the experiments, like measuring deflections of particles in a steady movement of the sample holder, developing better ways to prepare the samples (spacers on the cover slide, sealing the sample to prevent drying). In the future, it could be an interesting and novel method for studying the rheological properties of hydrogels.

Macro and microrheology offer different points of view on the same issues. They can be used as complementary methods, based on the goal of the analysis. Rheometry offers rapid and precise characterisation of viscoelastic properties, but only in a limited frequency range. Microrheological methods can be used to extend this range and provide useful insights, but their limitations and possible inaccuracies need to be kept in mind.

7 REFERENCES

[1] BARNES, H. A.; HUTTON, J. F. a WALTERS, Ken. An introduction to rheology. Amsterdam: Elsevier, c1989. ISBN 04-448-7140-3.

[2] MEZGER, Thomas G. Applied rheology. 6th edition. Austria: Anton Paar, 2019. ISBN 978-39504016-0-8.

[3] *Basics of rheology*. Online. In: Anton Paar. Dostupné z: https://wiki.anton-paar.com/en/basics-of-rheology/#introduction-to-rheology. [cit. 2024-02-05].

[4] HOLUBOVÁ, Renata. Základy reologie a reometrie kapalin. Olomouc: Univerzita Palackého v Olomouci, 2014. ISBN 978-80-244-41

[5] LUIS VELÁZQUEZ ORTEGA, José. Bingham Fluid Simulation in Porous Media with Lattice Boltzmann Method. Online. *Computational Fluid Dynamics Simulations*. 2020. ISBN 978-1-83880-749-8. Dostupné z: https://doi.org/10.5772/intechopen.90167. [cit. 2024-02-11].

[6] MEWIS, Jan a WAGNER, Norman J. Thixotropy. Online. *Advances in Colloid and Interface Science*. 2009, roč. 147-148, s. 214-227. ISSN 00018686. Dostupné z: https://doi.org/10.1016/j.cis.2008.09.005. [cit. 2024-02-13].

[7] OATES, Katherine M.N; KRAUSE, Wendy E; JONES, Ronald L a COLBY, Ralph H. Rheopexy of synovial fluid and protein aggregation. Online. *Journal of The Royal Society Interface*. 2006, roč. 3, č. 6, s. 167-174. ISSN 1742-5689. Dostupné z: https://doi.org/10.1098/rsif.2005.0086. [cit. 2024-02-13].

[8] *Hooke's law*. Online. In: Britannica. 2023. Dostupné z: https://www.britannica.com/science/Hookes-law. [cit. 2024-02-11].

[9] EDGEWORTH, R; DALTON, B J a PARNELL, T. The pitch drop experiment. Online. *European Journal of Physics*. 1984, roč. 5, č. 4, s. 198-200. ISSN 0143-0807. Dostupné z: https://doi.org/10.1088/0143-0807/5/4/003. [cit. 2024-02-05].

[10] A Basic Introduction to Rheology. In: Malvern Panalytical [online]. [cit. 2024-04-22]. Dostupné z: https://cdn.technologynetworks.com/TN/Resources/PDF/WP160620BasicIntroRheology.pdf

[11] Dealy, J. & Plazek, Donald. (2009). Time-temperature superposition-a users guide. Rheol. Bull.. 78. 16-31.

[12] XIA, Qiuyang; XIAO, Huining; PAN, Yuanfeng a WANG, Lidong. Microrheology, advances in methods and insights. Online. *Advances in Colloid and Interface Science*. 2018, roč. 257, s. 71-85. ISSN 00018686. Dostupné z: https://doi.org/10.1016/j.cis.2018.04.008. [cit. 2024-01-17].

[13] MANSEL, Bradley W.; KEEN, Stephen; PATTY, Philipus J.; HEMAR, Yacine a WILLIAMS, Martin. A Practical Review of Microrheological Techniques. Online. *Rheology - New Concepts, Applications and Methods*. 2013. ISBN 978-953-51-0953-2. Dostupné z: https://doi.org/10.5772/53639. [cit. 2024-02-27].

[14] DUFFY, John; REGA, Carlos; JACK, Robert a AMIN, Samiul. An Algebraic Approach for Determining Viscoelastic Moduli from Creep Compliance through Application of the Generalised Stokes-Einstein Relation and Burgers Model. Online. *Applied rheology*. 2016, roč. 26, č. 15130. Dostupné z: https://doi.org/10.3933/ApplRheol-26-15130. [cit. 2024-04-22].

[15] SQUIRES, Todd M. Nonlinear Microrheology: Bulk Stresses versus Direct Interactions. Online. *Langmuir*. 2008, roč. 24, č. 4, s. 1147-1159. ISSN 0743-7463. Dostupné z: https://doi.org/10.1021/la7023692. [cit. 2024-01-24]

[16] WIRTZ, Denis. Particle-Tracking Microrheology of Living Cells: Principles and Applications. Online. *Annual Review of Biophysics*. 2009, roč. 38, č. 1, s. 301-326. ISSN 1936-122X. Dostupné z: https://doi.org/10.1146/annurev.biophys.050708.133724. [cit. 2024-04-13].
[17] STETEFELD, Jörg; MCKENNA, Sean A. a PATEL, Trushar R. Dynamic light scattering: a practical guide and applications in biomedical sciences. Online. *Biophysical Reviews*. 2016, roč. 8, č. 4, s. 409-427. ISSN 1867-2450. Dostupné z: https://doi.org/10.1007/s12551-016-0218-6. [cit. 2024-01-17].
[18] *The principles of dynamic light scattering*. Online. In: Anton Paar. Dostupné z: https://wiki.anton-paar.com/en/the-principles-of-dynamic-light-scattering/. [cit. 2024-02-29].
[19] JOYNER, Katherine; YANG, Sydney a DUNCAN, Gregg A. Microrheology for biomaterial design. Online. *APL Bioengineering*. 2020, roč. 4, č. 4. ISSN 2473-2877. Dostupné z: https://doi.org/10.1063/5.0013707. [cit. 2024-02-19].
[20] CAI, Pamela C.; KRAJINA, Brad A.; KRATOCHVIL, Michael J.; ZOU, Lei; ZHU, Audrey et al. Dynamic light scattering microrheology for soft and living materials. Online. *Soft Matter*. 2021, roč. 17, č. 7, s. 1929-1939. ISSN 1744-683X. Dostupné z: https://doi.org/10.1039/D0SM01597K. [cit. 2024-02-29].
[21] MAGDE, Douglas; ELSON, Elliot a WEBB, W. W. Thermodynamic Fluctuations in a Reacting System—Measurement by Fluorescence Correlation Spectroscopy. Online. *Physical Review Letters*. 1972, roč. 29, č. 11, s. 705-708. ISSN 0031-9007. Dostupné z: https://doi.org/10.1103/PhysRevLett.29.705. [cit. 2024-01-24].
[22] SHUSTERMAN, Roman; ALON, Sergey; GAVRINYOV, Tatyana a KRICHEVSKY, Oleg. Monomer Dynamics in Double- and Single-Stranded DNA Polymers. Online. *Physical Review Letters*. 2004, roč. 92, č. 4. ISSN 0031-9007. Dostupné z: https://doi.org/10.1103/PhysRevLett.92.048303. [cit. 2024-04-22].
[23] SCHWILLE, Petra a HAUSTEIN, Elke. Fluorescence Correlation Spectroscopy - An Introduction to its Concepts and Applications. Online. *Spectroscopy*. 2001, roč. 2001, č. 94(22). Dostupné z: https://www.biophysics.org/Portals/0/BPSAssets/Articles/schwille.pdf. [cit. 2024-01-24].
[24] KOYNOV, Kaloian a BUTT, Hans-Jürgen. Fluorescence correlation spectroscopy in colloid and interface science. Online. 2012, roč. 17, č. 6, s. 377-387. ISSN 13590294. Dostupné z: https://doi.org/10.1016/j.cocis.2012.09.003. [cit. 2024-02-27].
[25] ELSON, Elliot L. Fluorescence Correlation Spectroscopy: Past, Present, Future. Online. *Biophysical Journal*. 2011, roč. 101, č. 12, s. 2855-2870. ISSN 00063495. Dostupné z: https://doi.org/10.1016/j.bpj.2011.11.012. [cit. 2024-01-24].
[26] BUSTAMANTE, Carlos J.; CHEMLA, Yann R.; LIU, Shixin a WANG, Michelle D. Optical tweezers in single-molecule biophysics. Online. *Nature Reviews Methods Primers*. 2021, roč. 1, č. 1. ISSN 2662-8449. Dostupné z: https://doi.org/10.1038/s43586-021-00021-6. [cit. 2024-02-14].
[27] ASHKIN, A.; DZIEDZIC, J. M.; BJORKHOLM, J. E. a CHU, Steven. Observation of a single-beam gradient force optical trap for dielectric particles. Online. *Optics Letters*. 1986, roč. 11, č. 5. ISSN 0146-9592. Dostupné z: https://doi.org/10.1364/OL.11.000288. [cit. 2024-02-14].
[28] VOLPE, Giovanni; MARAGÒ, Onofrio M; RUBINSZTEIN-DUNLOP, Halina; PESCE, Giuseppe; STILGOE, Alexander B et al. Roadmap for optical tweezers. Online. *Journal of Physics: Photonics*. 2023, roč. 5, č. 2. ISSN 2515-7647. Dostupné z: https://doi.org/10.1088/2515-7647/acb57b. [cit. 2024-02-29].

[29] TASSIERI, Manlio; EVANS, R M L; WARREN, Rebecca L; BAILEY, Nicholas J a COOPER, Jonathan M. Microrheology with optical tweezers: data analysis. Online. *New Journal of Physics*. 2012, roč. 14, č. 11. ISSN 1367-2630. Dostupné z: https://doi.org/10.1088/1367-2630/14/11/115032. [cit. 2024-03-11].

[30] BRAU, R R; FERRER, J M; LEE, H; CASTRO, C E; TAM, B K et al. Passive and active microrheology with optical tweezers. Online. *Journal of Optics A: Pure and Applied Optics*. 2007, roč. 9, č. 8, s. S103-S112. ISSN 1464-4258. Dostupné z: https://doi.org/10.1088/1464-4258/9/8/S01. [cit. 2024-04-11].

[31] CARTER, Brian C; SHUBEITA, George T a GROSS, Steven P. Tracking single particles: a user-friendly quantitative evaluation. Online. *Physical Biology*. 2005, roč. 2, č. 1, s. 60-72. ISSN 1478-3967. Dostupné z: https://doi.org/10.1088/1478-3967/2/1/008. [cit. 2024-04-13].

[32] HO, Tzu-Chuan; CHANG, Chin-Chuan; CHAN, Hung-Pin; CHUNG, Tze-Wen; SHU, Chih-Wen et al. Hydrogels: Properties and Applications in Biomedicine. Online. *Molecules*. 2022, roč. 27, č. 9. ISSN 1420-3049. Dostupné z: https://doi.org/10.3390/molecules27092902. [cit. 2024-01-31].

[33] HOFFMAN, Allan S. Hydrogels for biomedical applications. Online. *Advanced Drug Delivery Reviews*. 2012, roč. 64, s. 18-23. ISSN 0169409X. Dostupné z: https://doi.org/10.1016/j.addr.2012.09.010. [cit. 2024-01-31].

[34] WICHTERLE, O. a LÍM, D. Hydrophilic Gels for Biological Use. Online. *Nature*. 1960, roč. 185, č. 4706, s. 117-118. ISSN 0028-0836. Dostupné z: https://doi.org/10.1038/185117a0. [cit. 2024-01-31].

[35] LI, Jianyu a MOONEY, David J. Designing hydrogels for controlled drug delivery. Online. *Nature Reviews Materials*. 2016, roč. 1, č. 12. ISSN 2058-8437. Dostupné z: https://doi.org/10.1038/natrevmats.2016.71. [cit. 2024-01-31].

[36] LIANG, Yongping; HE, Jiahui a GUO, Baolin. Functional Hydrogels as Wound Dressing to Enhance Wound Healing. Online. *ACS Nano*. 2021, roč. 15, č. 8, s. 12687-12722. ISSN 1936-0851. Dostupné z: https://doi.org/10.1021/acsnano.1c04206. [cit. 2024-01-31].

[37] SMIDSRØD, Olav a MOE, Størker. *Biopolymer Chemistry*. Tapir Academic Press, 2008. ISBN 978-82-519-2384-2.

[38] LEE, Pei Yun; COSTUMBRADO, John; HSU, Chih-Yuan a KIM, Yong Hoon. Agarose Gel Electrophoresis for the Separation of DNA Fragments. Online. *Journal of Visualized Experiments*. 2012, č. 62. ISSN 1940-087X. Dostupné z: https://doi.org/10.3791/3923. [cit. 2024-03-13].

[39] YAZDI, Mohsen Khodadadi; TAGHIZADEH, Ali; TAGHIZADEH, Mohsen; STADLER, Florian J.; FAROKHI, Mehdi et al. Agarose-based biomaterials for advanced drug delivery. Online. *Journal of Controlled Release*. 2020, roč. 326, s. 523-543. ISSN 01683659. Dostupné z: https://doi.org/10.1016/j.jconrel.2020.07.028. [cit. 2024-03-13].

[40] ZARRINTAJ, Payam; MANOUCHEHRI, Saeed; AHMADI, Zahed; SAEB, Mohammad Reza; URBANSKA, Aleksandra M. et al. Agarose-based biomaterials for tissue engineering. Online. *Carbohydrate Polymers*. 2018, roč. 187, s. 66-84. ISSN 01448617. Dostupné z: https://doi.org/10.1016/j.carbpol.2018.01.060. [cit. 2024-03-13].

[41] VEN, Seow a RANI, Abdul. Discriminatory Power of Agarose Gel Electrophoresis in DNA Fragments Analysis. Online. *Gel Electrophoresis - Principles and Basics*. 2012. ISBN 978-953-51-0458-2. Dostupné z: https://doi.org/10.5772/36891. [cit. 2024-03-20].

[42] IURCIUC, Camelia Elena; SAVIN, A.; LUNGU, C.; MARTIN, P. a POPA, M. Gellan. Food applications. Online. *Cellulose Chemistry and Technology*. Roč. 2015, č. 50. Dostupné z: https://cellulosechemtechnol.ro/pdf/CCT1(2016)/p.1-13.pdf. [cit. 2024-03-20].

[43] OSMAŁEK, Tomasz; FROELICH, Anna a TASAREK, Sylwia. Application of gellan gum in pharmacy and medicine. Online. *International Journal of Pharmaceutics*. 2014, roč. 466, č. 1-2, s. 328-340. ISSN 03785173. Dostupné z: https://doi.org/10.1016/j.ijpharm.2014.03.038. [cit. 2024-03-20].

[44] VALDEZ, Juanita; GALINDO, Aidé; BADILLO, Claudia; FACIO, Adali a VASQUEZ, Pablo. Hydroxyapatite and Biopolymer Composites with Promising Biomedical Applications. Online. *Revista Mexicana de Ingeniería Biomédica*. 2022, č. 43(2). Dostupné z: https://doi.org/10.17488/RMIB.43.2.1. [cit. 2024-03-20].

[45] GUIGAS, Gernot; KALLA, Claudia a WEISS, Matthias. Probing the Nanoscale Viscoelasticity of Intracellular Fluids in Living Cells. Online. *Biophysical Journal*. 2007, roč. 93, č. 1, s. 316-323. ISSN 00063495. Dostupné z: https://doi.org/10.1529/biophysj.106.099267. [cit. 2023-12-04].

[46] RATHGEBER, Silke; BEAUVISAGE, Hans-Josef; CHEVREAU, Hubert; WILLENBACHER, Norbert a OELSCHLAEGER, Claude. Microrheology with Fluorescence Correlation Spectroscopy. Online. *Langmuir*. 2009, roč. 25, č. 11, s. 6368-6376. ISSN 0743-7463. Dostupné z: https://doi.org/10.1021/la804170k. [cit. 2023-12-04].

[47] KRAJINA, Brad A.; TROPINI, Carolina; ZHU, Audrey; DIGIACOMO, Philip; SONNENBURG, Justin L. et al. Dynamic Light Scattering Microrheology Reveals Multiscale Viscoelasticity of Polymer Gels and Precious Biological Materials. Online. *ACS Central Science*. 2017, roč. 3, č. 12, s. 1294-1303. ISSN 2374-7943. Dostupné z: https://doi.org/10.1021/acscentsci.7b00449. [cit. 2024-02-19].

[48] WEIHS, Daphne; MASON, Thomas G. a TEITELL, Michael A. Bio-Microrheology: A Frontier in Microrheology. Online. *Biophysical Journal*. 2006, roč. 91, č. 11, s. 4296-4305. ISSN 00063495. Dostupné z: https://doi.org/10.1529/biophysj.106.081109. [cit. 2024-02-29].

[49] OPPONG, Felix K.; RUBATAT, Laurent; FRISKEN, Barbara J.; BAILEY, Arthur E. a DE BRUYN, John R. Microrheology and structure of a yield-stress polymer gel. Online. *Physical Review E*. 2006, roč. 73, č. 4. ISSN 1539-3755. Dostupné z: https://doi.org/10.1103/PhysRevE.73.041405. [cit. 2024-01-24].

[50] TASSIERI, Manlio; GIBSON, Graham M.; EVANS, R. M. L.; YAO, Alison M.; WARREN, Rebecca et al. Measuring storage and loss moduli using optical tweezers: Broadband microrheology. Online. *Physical Review E*. 2010, roč. 81, č. 2. ISSN 1539-3755. Dostupné z: https://doi.org/10.1103/PhysRevE.81.026308. [cit. 2024-03-11].

[51] PESCE, G; DE LUCA, A C; RUSCIANO, G; NETTI, P A; FUSCO, S et al. Microrheology of complex fluids using optical tweezers: a comparison with macrorheological measurements. Online. *Journal of Optics A: Pure and Applied Optics*. 2009, roč. 11, č. 3. ISSN 1464-4258. Dostupné z: https://doi.org/10.1088/1464-4258/11/3/034016. [cit. 2024-03-25].

[52] HNYLUCHOVÁ, Z. Mikroreologie biokoloidních systémů. Brno: Vysoké učení technické v Brně, Fakulta chemická, 2016. 137 s. (přílohy 17 s.). Vedoucí dizertační práce: prof. Ing. Miloslav Pekař, CSc.

[53] MONDEK, J. Časově rozlišená fluorescence ve výzkumu interakcí hyaluronanu a koloidních systémů. Brno: Vysoké učení technické v Brně, Fakulta chemická, 2018. 162 s. Vedoucí dizertační práce prof. Ing. Miloslav Pekař, CSc.

[54] PÍŠOVÁ, D. Studium transportních procesů v hydrogelech pomocí mikroreologickýchtechnik. Brno: Vysoké učení technické v Brně, Fakulta chemická, 2017. 70 s. Vedoucí diplomové práce Ing. Jiří Smilek, Ph.D.
[55] KÁBRTOVÁ, P. Pokročilé mikroreologické techniky ve výzkumu hydrogelů. Brno: Vysoké učení technické v Brně, Fakulta chemická, 2017. 63 s. Vedoucí diplomové práce Ing. Filip Mravec, Ph.D.

8 LIST OF ABBREVIATIONS AND SYMBOLS

8.1 Abbreviations

DLS	Dynamic light scattering
FCS	Fluorescence correlation spectroscopy
GSER	Generalised Stokes-Einstein relation
HA	Hyaluronic acid
LVE region	Linear viscoelastic region
MPT	Multiple particle tracking
MSD	Mean-square displacement
OT	Optical tweezers
PAM	polyacrylamide
PS	Polystyrene
PTM	Particle tracking microrheology
TTS	Time-temperature superposition

8.2 Symbols

F	force	[N]
v	velocity	[m/s]
τ	shear stress	[Pa]
A	area	[m^2]
$\dot{\gamma}$	shear rate	[s^{-1}]
h	gap height	[m]
η	viscosity	[Pa·s]
ν	kinematic viscosity	[m^2/s]
ρ	density	[kg/m^3]
D_e	Deborah number	[-]
t	time	[s]
s	deflection path	[m]
γ	shear strain	[-]
G	shear modulus	[Pa]
f	frequency	[Hz]
ω	angular frequency	[rad/s]
δ	phase shift	[°]
G^*	complex shear modulus	[Pa]
G'	storage modulus	[Pa]
G''	loss modulus	[Pa]
J	creep compliance	[Pa^{-1}]
T	temperature	[K]
r	radius	[m]
$\langle \Delta r^2(t) \rangle$	mean square displacement	[m^2]
G(t)	autocorrelation function	[-]
N	average number of species in volume	[-]
w_{xy}, w_z	dimensions of the confocal volume	[m]

τ_D	diffusion time	[s]
V_{eff}	effective volume	[m^3]
D	diffusion coefficient	[m^2/s]
r_0	radius of confocal volume	[m]
κ	optical trap stiffness	[N/m]

9 APPENDIX

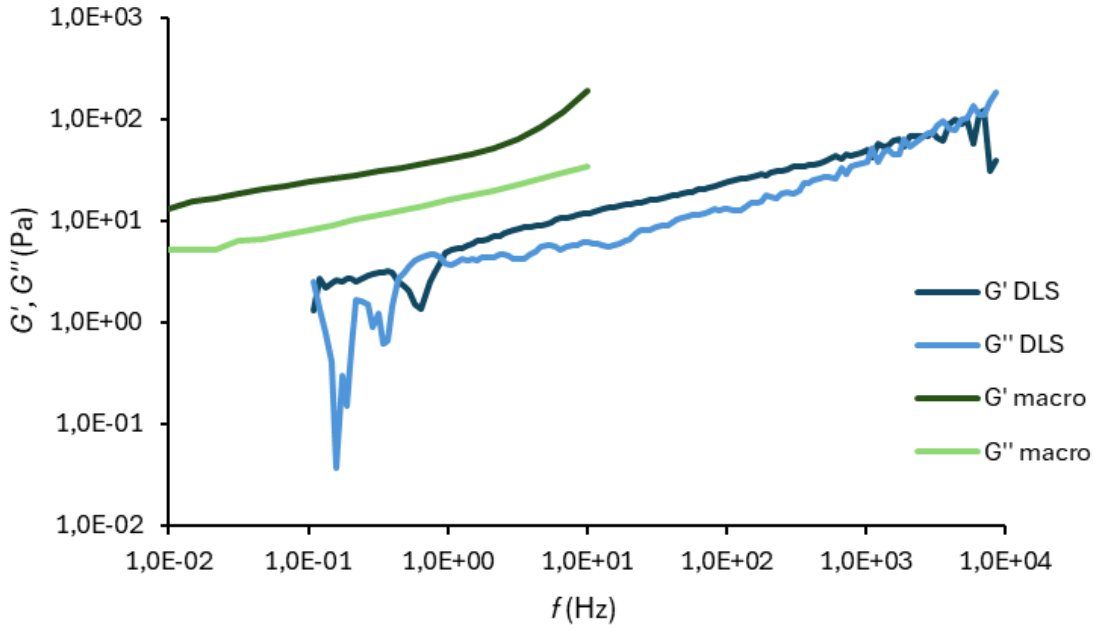

Figure 36 Comparison of viscoelastic moduli from DLS and from rheometry for 1% gellan at 25 °C

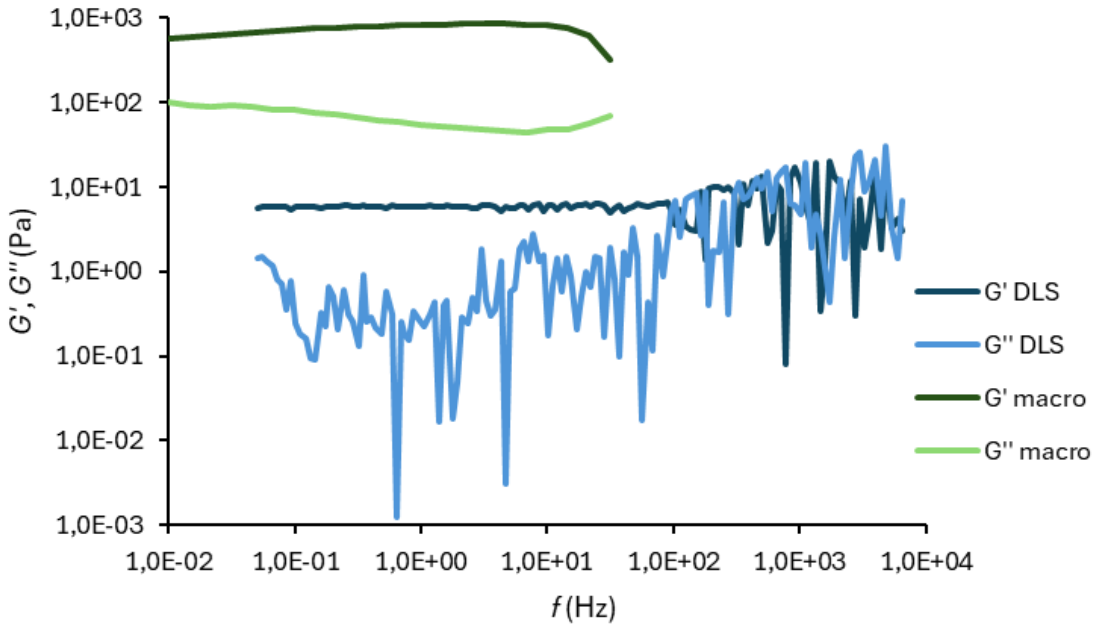

Figure 37 Comparison of viscoelastic moduli from DLS and from rheometry for 0.5% agarose at 25 °C

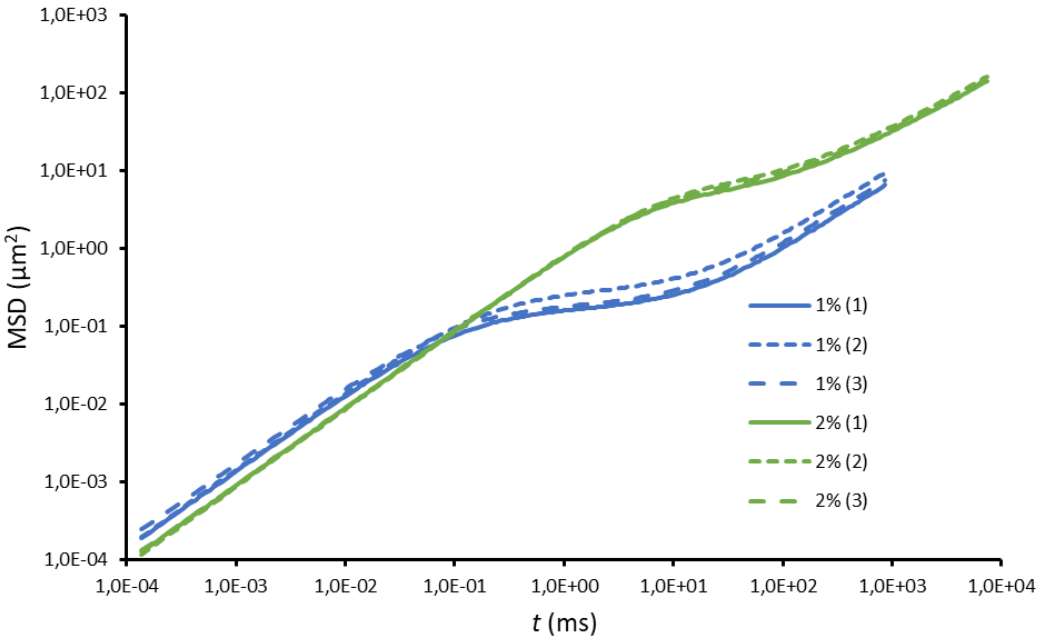

Figure 38 MSD curves for gellan hydrogels obtained from FCS

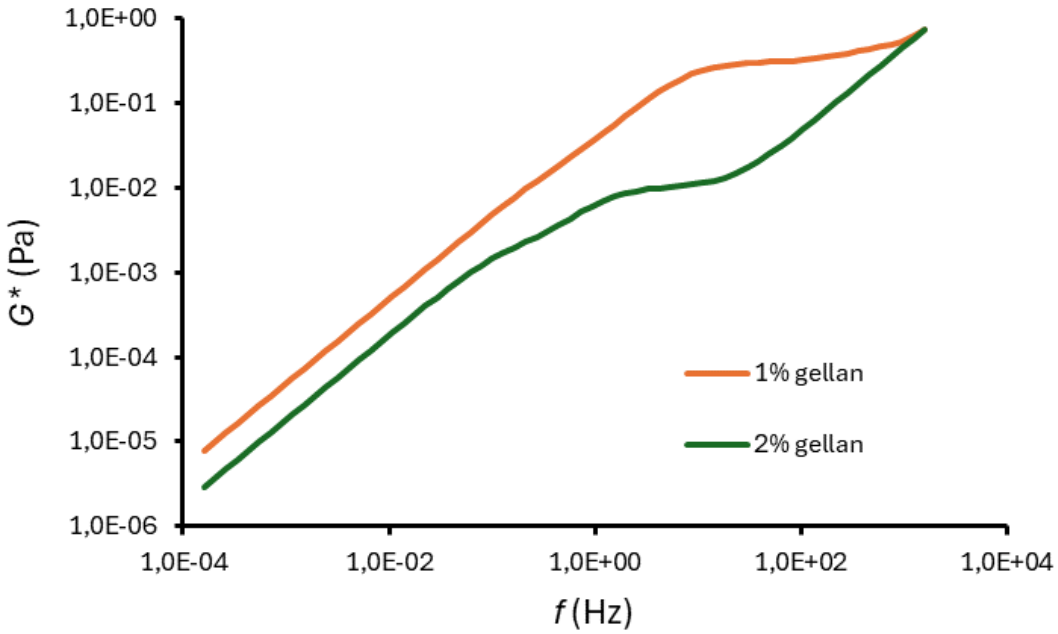

Figure 39 Comparison of complex modulus for gellan hydrogels from FCS

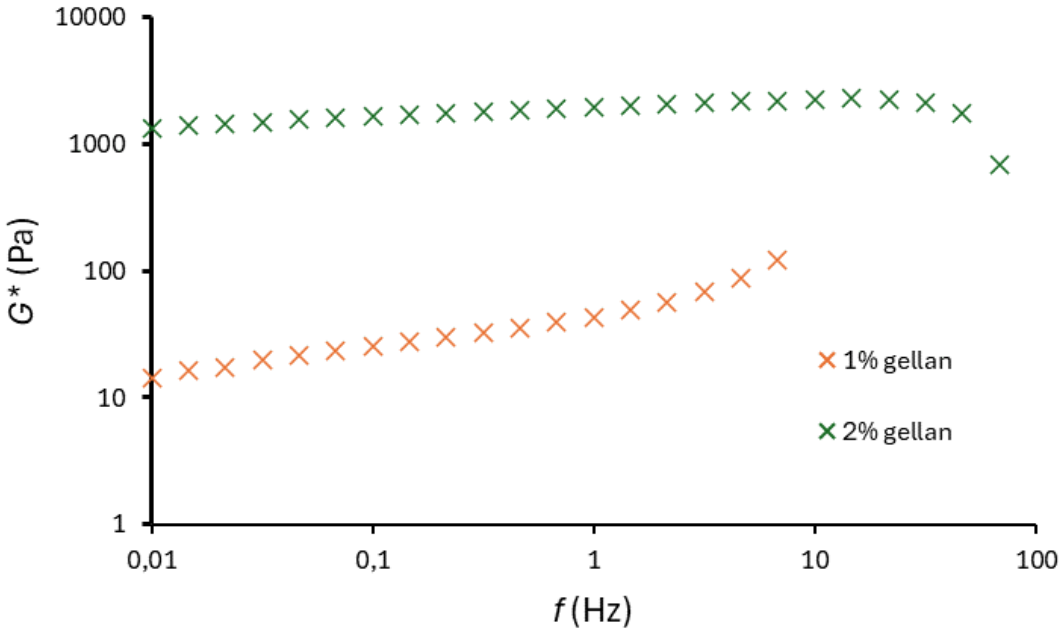

Figure 40 Comparison of G for gellan gels from rheometry*

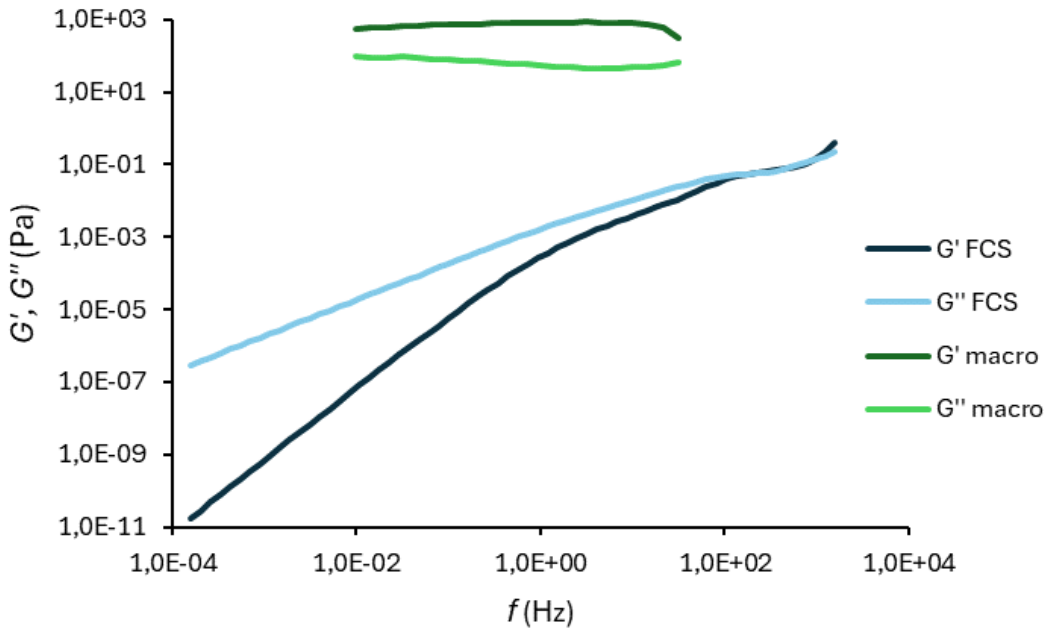

Figure 41 Comparison of viscoelastic moduli of 0.5% agarose gel obtained by FCS and macrorheology

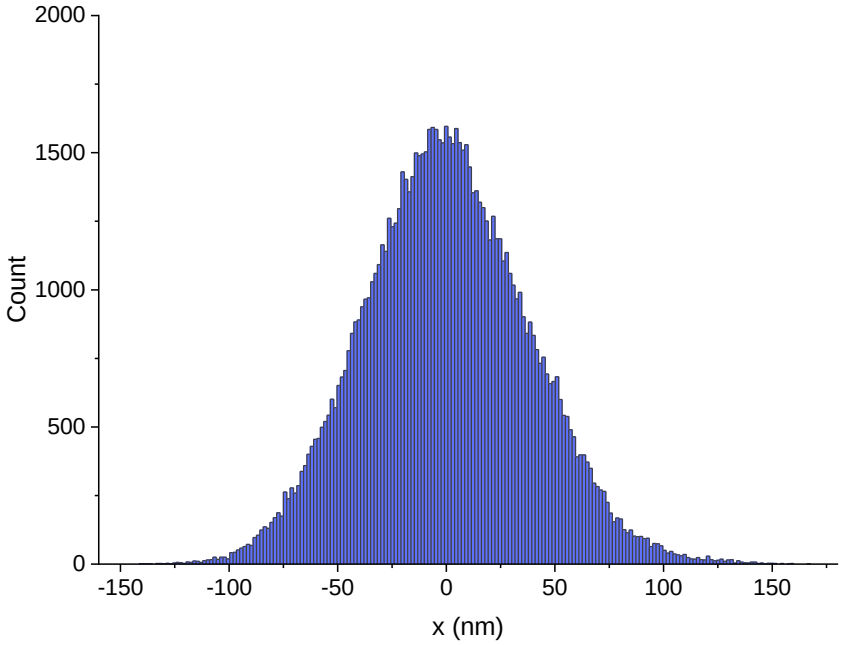

Figure 42 Histogram of deflections of a trapped probe in 75% glycerol solution

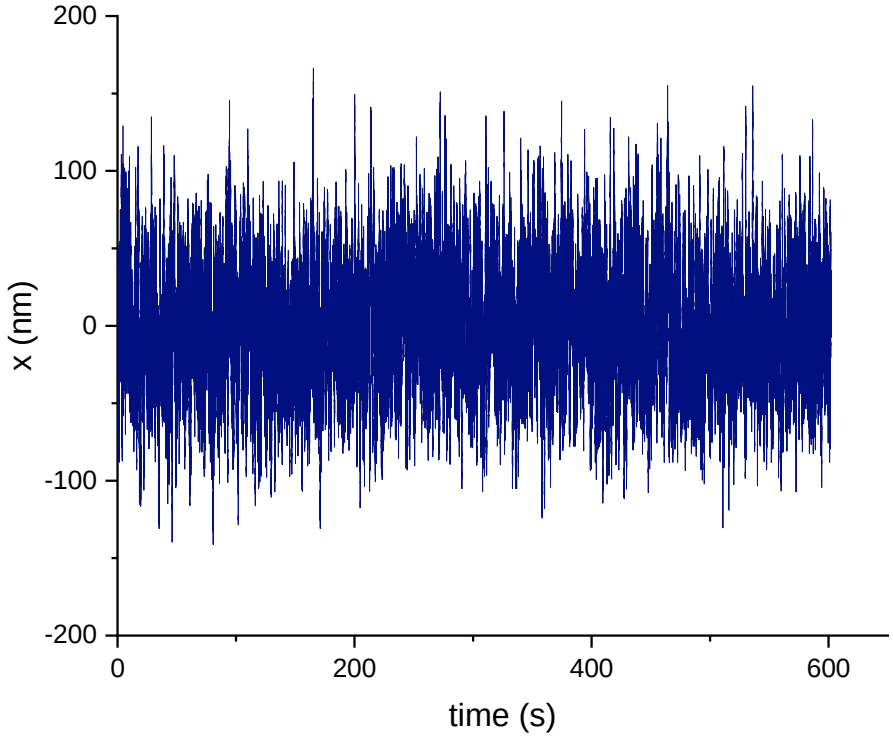

Figure 43 Time-dependence of the position of a trapped particle in 75% glycerol solution